

Department of Agrarbiotechnology, IFA-Tulln
Institute of Environmental Biotechnology

Master thesis

To obtain the academic degree of Dipl.-Ing. at the University of
Natural Resources and Life Sciences, Vienna

Characterization of immobilized *Humicola insolens*
Cutinase

Submitted by:

Julian Loibl B.Sc.

October 2017, Vienna

Supervisors:

Univ. Prof. DI Dr. Georg Gübitz

Dr. Enrique Herrero Acero

Felice Quartinello, M.Sc.

Abstract

Polyesters, especially polyethylene terephthalate (PET), are widespread in many daily applications, including the textile industry. Due to their resistance to degradation, textile waste is landfilled, incinerated or – preferably - recycled. Novel recycling processes refer to biocatalysis-based technologies for plastic textile waste preprocessing, ink removal and hydrolysis while keeping energy costs low. Such technologies apply cutinases, enzymes that are produced in plant pathogenic fungi and bacteria, which can degrade the natural plant polymer cutin as well as artificial polymers like PET, making these biocatalysts interesting for industrial applications.

This master thesis concentrates focuses to on the improvement of the recycling process for synthetic fiber based textiles targeting an optimization of reaction conditions for immobilized enzymes to achieve optimal performance. The very target of this work was the immobilization of *Humicola insolens* cutinase on SEPABEADSTMECEP/M (Resindion), for hydrolysis of PET powder, its oligomers such as bis(2-hydroxyethyl) terephthalate (BHET) or bis(benzoyloxyethyl) terephthalate (3-PET) and applying optimized parameters for enzymatic treatment of chemically preprocessed PET fiber samples.

The overall-performance of the immobilized cutinase was explored under different experimental conditions and compared to the free enzyme. A higher concentration of released monomers was verified under alkaline conditions simultaneously with increased enzyme activity in the supernatant. The performance improved when using the model substrates 3-PET and the water-soluble BHET. The best result was achieved with chemically preprocessed samples at pH 7 and 50°C.

Free cutinase performed sufficiently under all conditions. The distribution of the hydrolysis products varied, depending on the pH level and incubation temperature. The percentage of released TA was highest at acidic conditions (pH 5.5) and 70°C. BHET was not stable when incubated at pH 8.5.

Zusammenfassung

Polyester, vor allem Polyethylen-Terephthalat oder PET sind Materialien mit verschiedensten Anwendungsmöglichkeiten, unter anderem in der Textilindustrie. Kunstfaserabfälle sind nicht abbaubar und müssen daher, deponiert, verbrannt oder – bevorzugter Weise - recycelt werden. Moderne Recycling-Konzepte nutzen Biokatalysator-basierte Technologien für Vorbehandlung, Entfärbung und Abbau von Kunststoffabfall unter vergleichsweise milden Reaktionsbedingungen.

Die, in pflanzenpathogenen Bakterien und Pilzen vorkommenden, Cutinasen sind in der Lage synthetische Polymere wie PET abzubauen, was diese Enzyme für umweltspezifische Anwendungen interessant macht.

Diese Masterarbeit konzentriert sich auf die Verbesserung des Recyclingprozesses für synthetische Textilien, mit dem Ziel die Reaktionsbedingungen für PET Hydrolyse mittels immobilisierter Cutinase zu optimieren. Die konkrete Aufgabe dieser Arbeit war die Immobilisierung von *Humicola insolens* Cutinase auf SEPABEADS™ ECEP / M (Resindion), zur Hydrolyse von pulverförmigen PET, dem beim Abbau entstehenden Bis (2-hydroxyethyl) terephthalat (BHET) und Bis (benzoyloxyethyl) terephthalat (3PET) um mit optimierten Reaktionsparametern die Abbaubarkeit von mit Druck und Hitze vorbehandelten PET Fasern zu testen.

Die generelle Performance der immobilisierten Cutinase wurde unter unterschiedlichen Reaktionsbedingungen getestet und direkt mit der des freien Enzyms verglichen. Bei Inkubation mit 3PET und wasserlöslichem BHET war die Konzentration an Reaktionsprodukten deutlich höher. BHET erwies sich als nicht stabil unter alkalischen Reaktionsbedingungen (pH 8.5). Die höchste Konzentration an freigesetzten Hydrolyseprodukten wurde bei vorbehandelten PET Fasern bei pH 7 und 50°C erzielt. Die freie Cutinase zeigte hohe Aktivität unter fast allen Bedingungen, wobei die Menge an freigesetzten Monomeren nach pH-Wert variierte. Der Anteil von freigesetztem TA war bei pH 5.5 und 70°C am höchsten.

Acknowledgement

Firstly, I would like to thank Univ.Prof. Dipl.-Ing. Dr.techn. Georg Gübitz for giving me the opportunity pursue my own ideas and interests and taking time to discuss my ideas and goals. I also want to thank Dr. Enrique Herrero-Acero for his guidance regarding the development of my research goals and especially Felice Quartinello, MSc. who helped and supported me continuously during and after my time at the IFA.

I want to thank my parents Celine and Wolfgang Loibl supporting during my long journey as a student as well as my siblings David and Lisa and my best Friend Philip.

Finally, I want to thank my wife Yarida for supporting and encouraging me so patiently and affectionately to finalize this project.

Abbreviations

Table 1: Abbreviations

BHET	Bis (Hydroxyethylene terephthalate)
BSA	Bovine serum albumine
RP-HPLC	Reverse phase High Performance Liquid Chromatography
HiC	<i>Humicola insolens</i> cutinase
fHiC	free <i>Humicola insolens</i> cutinase
iHiC	immobilized <i>Humicola insolens</i> cutinase
EC/EP	Enzyme carrier with epoxy functional group
FT-IR	Fouriertransform Infrared spectroscopy
K-Pi	Potassium phosphate
MQ	MilliQ-Water
MHET	Mono (Hydroxyethylene terephthalate)
NaAc	Sodium acetate
PEG	Polyethylene terephthalate
3-PET	Bis(benzoyloxyethyl) terephthalate
<i>p</i> -NPA	para-nitrophenylacetate
<i>p</i> -NPB	para-nitrophenylbutyrate
SDS-PAGE	Sodiumdodecyl-polyacrylamide gelelectrophoresis
SN	Supernatant
STD	Standard deviation
TA	Terephthalic acid
p-TA	purified terephthalic acid

Table of Contents

Department of Agrarbiotechnology, IFA-Tulln Institute of Environmental Biotechnology	
Master thesis.....	
Abstract	i
Zusammenfassung	ii
Acknowledgement.....	iii
Abbreviations	iv
Table of Contents	v
Table of figures	vii
Table of equations	x
1. Introduction	1
1.1. Outline of this work.....	1
1.2. α/β Hydrolases.....	1
1.2.1. Cutinases	3
1.3. Green chemistry	5
1.4. Poly ethylene terephthalate	6
1.4.1. Application of PET for synthetic fiber production.....	7
1.4.2. Chemical and Mechanical recycling	8
1.4.3. Other recycling techniques	9
1.5. The RESYNTEX project.....	9
1.5.1. Work package 4.....	12
1.6. Immobilization of enzymes	12
1.6.1. Carrier bound immobilization	13
1.6.2. Entrapment	15
1.6.3. Cross-linking	15
2. Materials.....	17
2.1. Buffers.....	17
2.2. SDS-PAGE.....	17

2.3.	Immobilization	17
2.4.	Determination of protein concentration.....	17
2.5.	Determination of enzyme activity	17
2.6.	Analysis of Substrate and Monomers	18
3.	Methods	19
3.1.	Bradford assay.....	19
3.2.	SDS- PAGE.....	19
3.3.	Fourier Transform Infrared(FT-IR) spectroscopy	20
3.4.	para-(Nitrophenyl substrate) activity assay	20
3.4.1.	Activity of free enzyme	20
3.4.2.	Activity of immobilized enzyme	21
3.5.	Immobilization	21
3.6.	Optimization of reaction conditions	22
3.6.1.	Long time stability.....	23
3.6.2.	Washing stability	23
3.6.3.	pH stability	24
3.6.4.	Influence of shaking	24
3.6.5.	Incubation with chemically preprocessed substrates	24
3.7.	RP- HPLC	25
3.7.1.	Calibration curve	25
3.7.2.	Sample preparation.....	26
4.	Results and Discussion	27
4.1.	SDS-PAGE.....	27
4.2.	Activity and enzyme concentration	28
4.2.1.	Immobilization	28
4.2.2.	Activity of the immobilized enzyme	29
4.2.3.	Long time leaching activity	29
4.2.4.	pH dependent leaching and activity (p-NPB activity assay)	30
4.2.5.	pH dependent leaching and activity (p-NPA activity assay)	32

4.3.	FT-IR analysis	34
4.4.	RP-HPLC results	36
4.4.1.	Washing stability	36
4.4.2.	Long time stability.....	37
4.4.3.	pH stability	38
4.4.4.	Variation of substrate ratios.....	44
4.4.5.	Hydrolysis of 3-PET.....	45
4.4.6.	Hydrolysis of BHET.....	47
4.4.7.	Hydrolysis of Resyntex samples	48
5.	Conclusions and outlook	52
6.	Appendix	54
7.	Reference list.....	65

Table of figures

Figure 1: Schematic diagram of the α/β hydrolase fold (Ollis et al. 1990)	2
Figure 2: Figure: A Ca diagram of the nucleophile elbow of the α/β hydrolase fold enzymes. Shown are Acetylcholinesterase(AChE) - green, wheat carboxypeptidase II (CPW) -orange, diene lactone hydrolase (DLH) -white, haloalkane dehalogenase (HAL) - red, Lipase (GLP -yellow) and triacyl glycerol lipase (MLIP) – blue (Ollis et al. 1992).	3
Figure 3:A schematic drawing of the plant cell wall/cuticle complex of focusing on the main structural parts. (Yeats and Rose 2013).....	4
Figure 4:Cartoon model of Humicola insolens cutinase (Own image created with PyMol® software) ..	5
Figure 5: Global production of fossil energy from 1800 to 2010 (Höök et al. 2012)	5
Figure 6: Synthesis of PET using the dimethyl terephthalate process	6
Figure 7: Synthesis of PET using the terephthalic acid process.....	7
Figure 8: Process scheme PET production (HITACHI 1994).....	7
Figure 9: Used textile composition (Own diagram, data from SOEXGroup (Germany)).....	8
Figure 10: Core goals of the Resyntex project (Resyntex 2017).....	10
Figure 11: Processing steps from waste material to chemical feedstock and value added products (Resyntex 2017)	11
Figure 12: Detailed process scheme of Work package 4 (Resyntex 2017).....	12

Figure 13: Techniques for carrier bound immobilization (Cantone et al. 2013).....	14
Figure 14: Stick Model of Humicola insolens Cutinase (Own image created with PyMol® software) with highlighted lysines (orange sticks) and the active site (in blue: Serine 105, Histidine 173 and aspartic acid 160 (Kold et al. 2014)).....	15
Figure 15: Simplified reaction of crosslinking between amino groups and HiC lysine residues. R ¹ = Protein, R ² = Carrier	27
Figure 16: Gel scan of SDS-PAGE after Coomassie staining. a-1) HiC, Size standard, a-2) Protein Ladder PageRuler™	27
Figure 17: Monitoring of immobilization of HiC a) Enzyme concentration in the supernatant, b) Ration HiC immobilized (STD < 0.5%)	28
Figure 18: Released p-NP after incubation of p-NPB with iHiC.	29
Figure 19: Activity of iHiC in U/gBeads	29
Figure 20: Activity of leached enzyme after long time incubation without substrate at 50°C 100rpm. Additional incubation with substrate of 72h und same conditions.....	30
Figure 21: Enzyme activity of fHiC. Incubation at 50°C, 100 rpm.....	31
Figure 22: Activity of iHiC. Incubation at 50°C, 100 rpm.....	31
Figure 23: Activity of iHiC. Incubation at 70°C, 100 rpm.....	31
Figure 24: Activity of fHiC. Incubation at 50°C, 100 rpm.	32
Figure 25: Activity of fHiC. Incubation at 70°C, 100 rpm.	32
Figure 26: Activity of iHiC. Incubation at 50°C, 100 rpm. (p-NPA).....	33
Figure 27: Activity of fHiC. Incubation at 50°C, 0 rpm (p-NPA).	33
Figure 28: Activity of fHiC. Incubation at 50°C, 100 rpm. at 70°C, 100 rpm (p-NPA)	34
Figure 29: FT-IR spectra of Resyntex samples that were chemically preprocessed. EE21B) Filtrated and lyophilized solution obtained after chemical hydrolysis. EE21C) lyophilized solid residues after hydrolysis. Normalization area 2200-2000 cm ⁻¹	35
Figure 30: FT-IR spectra of PET powder and TA. Normalization area 2200-2000 cm ⁻¹	36
Figure 31: Effect of washing on hydrolytic activity of iHiC. a) Concentration MHET, b) specific product release MHET, c) chemical structure of MHET	37
Figure 32: Long time incubation of PET powder with iHiC 100 rpm, 50°C. a) Concentration TA/MHET, b) specific product release TA/MHET, additional incubation with substrate of 72h und same conditions (STD < 0.5%)	38
Figure 33: Incubation of PET with iHiC 100rpm, 50°C. a) Concentration TA/MHET, b) specific monomer release TA/MHET (no STD after 120h incubation time because of partial precipitation of monomers within sample triplicate)	39
Figure 34: Incubation of PET with iHiC at 0rpm, 50°C. a) Concentration TA/MHET, b) specific monomer release TA/MHET	40

Figure 35: Incubation of PET powder with iHiC at 100rpm, 70°C. a) Concentration TA/MHET, b) specific monomer release TA/MHET	41
Figure 36: Incubation of PET powder with fHiC at 100rpm, 50°C. a) Concentration TA/MHET, b) specific monomer release TA/MHET	42
Figure 37: Incubation of PET powder with fHiC at at 0rpm, 50°C. a) Concentration of released Monomers, b) specific monomer release TA/MHET	43
Figure 38: Incubation of PET powder with fHiC at 100rpm, 70°C. a) Concentration of released TA/MHET, b) specific monomer release TA/MHET	44
Figure 39: 2.5-20 mg of PET powder mixed with 10 mg of iHiC Substrate. Incubation with Tris/HCl 0.1M, pH 7 at 100rpm, 50°C	45
Figure 40: Chemical Structure of 3-PET	45
Figure 41: Incubation of 3-PET with iHiC at 100rpm, 50°C (no STD at pH 5.5 because of partial precipitation of monomers within sample triplicate).....	46
Figure 42: Incubation of 3-PET with fHiC at 100rpm, 50°C	46
Figure 43: Blank of 3-PET. Incubation at 100rpm, 50°C.....	46
Figure 44: Chemical structure of BHET	47
Figure 45: Incubation of BHET with iHiC at 100rpm, 50°C	47
Figure 46 Incubation of BHET with fHiC (100rpm, 50°C)	47
Figure 47: Blank-of BHET (100rpm, 50°C)	48
Figure 48: Blanks for incubation of chemically preprocessed PET fiber without filtration (EE21A). TA_B: Blank for TA (substrate + buffer). MHET_B: Blank for MHET. TA_B+B: Blank for TA + EC/EP beads, MHET_B+B: Blank für MHET + EC/EP beads	48
Figure 49: Blanks for incubation of chemically preprocessed PET fibre with filtration (EE21B). TA_B: Blank for TA (substrate + buffer). MHET_B: Blank for MHET. TA_B+B: Blank for TA + EC/EP beads, MHET_B+B: Blank für MHET + EC/EP beads	49
Figure 50: Incubation of lyophilized solution derived from chemically hydrolyzed PET fiber before filtration (EE21A) with iHiC at 100rpm, 50°C	49
Figure 51: Incubation of lyophilized solution derived from chemically hydrolyzed PET fiber after filtration (EE21B) with iHiC at 100rpm, 50°C	49
Figure 52: Incubation of lyophilized solution derived from chemically hydrolyzed PET fiber before filtration (EE21A) with fHiC at 100rpm, 50°C (no STD at pH 5.5 and 7 because of partial precipitation of monomers within sample triplicate).....	50
Figure 53: Incubation of lyophilized solution derived from chemically hydrolyzed PET fiber after filtration (EE21B) with fHiC at 100rpm, 50°C (no STD after 120h incubation time because of partial precipitation of monomers within triplicate).....	50
Figure 54: Reduction of disulfide bonds	55

Figure 55: Effect of SDS on polypeptide chains	55
Figure 56: Types of movement induced by infrared radiation (Alvarez-Ordóñez & Prieto 2012)	56
Figure 57: Basic components of an FT-IR spectrometer (Alvarez-Ordóñez and Prieto 2012).....	57
Figure 58: Hydrolysis of the substrate molecule	58
Figure 59: setup of a HPLC system (Waters 2017).....	59
Table 1: Abbreviations	iv
Table 2: The Resyntex work packages (Resyntex 2017)	11
Table 3: Alternative substrates for hydrolysis.....	25
Table 4: RP-HPLC gradient	25
Table 5: BSA calibration 1	57
Table 6: BSA calibration 2	58
Table 7: Standard calibration TA	59
Table 8: Standard calibration BHET	60

Table of equations

(1) Eq. 1: Calibration:.....	19
(2) Eq. 2: Activity free Enzyme	20
(3) Eq. 3: Activity immobilized enzyme	21
(4) Eq. 4: Immobilization efficiency	22
(5) Eq. 5: Weight iHiC	22
(6) Eq. 6: specific Hydrolysatation rate iHiC.....	23

1. Introduction

1.1. Outline of this work

The research concept of this master thesis can be split in two major parts, beginning with a characterization process for immobilized *Humicola insolens* cutinase hydrolyzing crystalline PET powder amongst other model substrates like bis-hydroxyethyl-terephthalate (BHET) and bis(benzoyloxyethyl) terephthalate (3-PET) to gain information on influence of reaction conditions towards efficacy of the enzyme. This was determined by measuring the concentration of released monomers such as TA or the oligomer BHET in the reaction buffer. This initial part is necessary to identify optimized reaction conditions for the second part of the thesis: The treatment of chemically preprocessed samples, where only PET oligomers were hydrolyzed and oligos from polyamide 6.6, which can be used as second value added chemicals were left out. Incubation with free enzyme was always performed under the same reaction conditions, since chemically preprocessed samples derived from the Resyntex project contain soluble as well as insoluble fractions, therefore incubation with free and immobilized enzyme finally gives a broader picture.

1.2. α/β Hydrolases

As one of the largest super-families, α/β Hydrolases and the structurally related enzymes belonging to this family show a broad repertoire of catalytic functions. In the beginning of the 1990's, the elucidation of the 3D-structures of five apparently unrelated hydrolytic enzymes revealed the so called α/β -hydrolase fold (Ollis et al. 1992). The examined enzymes were acetylcholine esterase (ACE) from *Torpedo californica* (Sussman et al. 1991), diene lactone hydrolase (DLH) from *Pseudomonas sp. B13* (Pathak and Ollis 1990), lipase (GCL) from *Geotrichum candidum* (Schrag et al. 1991), carboxypeptidase (WCP) from wheat (Liao D I and Remington 1990) and haloalkane dehalogenase (HAL) from *Xanthobacter autotrophicus* (Franken et al. 1991). "The canonical" α/β -hydrolase fold is an eight-stranded mostly parallel α/β structure. The fold has one strand (β_2) antiparallel to the rest with the connections of the strands as outlined in Figure 1. The sheet is bent to form a half-barrel and it is highly twisted with the first and last strand being oriented at approximately 90° angle to one another. The first and last helices, respectively, α_A and α_F are packed on one side of the sheet, while the rest of the helices are located on the opposite side of the sheet (Holmquist 2000).

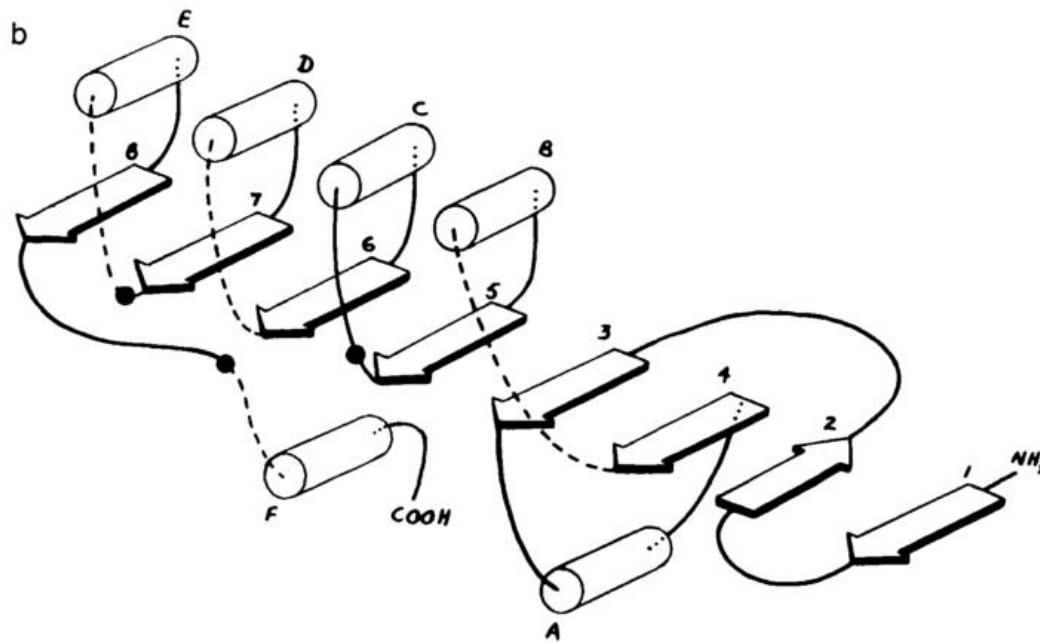


Figure 1: Schematic diagram of the α/β hydrolase fold (Ollis et al. 1990)

The α/β hydrolase fold marks the core of the enzyme. This structure contains the catalytic triad, as identified by Ollis. The active site loops like the “*nucleophilic elbow*”, which is the most preserved region has a central γ -shaped turn between strand five and helix C. The shape and degree of curvature of the β -sheet has a strong influence on large scale structural differences of α/β cores.

These nucleophilic amino acids are always found within a cavity, consisting usually of a penta peptide Gly-X-Ser-X-Gly. The function of this cavity is to contribute to the formation and stabilization of the oxyanion-hole, important for the stability.

Figure 2 shows the nucleophilic elbow region of several α/β Hydrolases. The high structural resemblance visualizes the importance of this area (Ollis et al. 1992). Together with the *acid turns* and the *histidine loop* the catalytic triad is formed. Cutinases show features of two enzyme classes containing this active center: Esterases which catalyze formation or hydrolysis of ester bonds and lipases which hydrolyze or synthesize lipids. Those proteins are closely related, although lipases have a unique structural feature called “lid” which covers the active site (Jaeger et al. 1999; Tyndall et al. 2002). In the closed state the active site maintains a hydrophobic state. This changes when the enzyme interacts with a lipid water bilayer interface, which leads the opening of the lid. Lipases can also be considered as esterases which act on long chain acetylgllycerols (Jaeger and Reetz 1998)

The geometry of the nucleophile elbow also contributes to the formation of the oxyanion-binding site, which is needed to stabilize the negatively charged transition state that occurs during hydrolysis (Nardini and Bauke 1999).

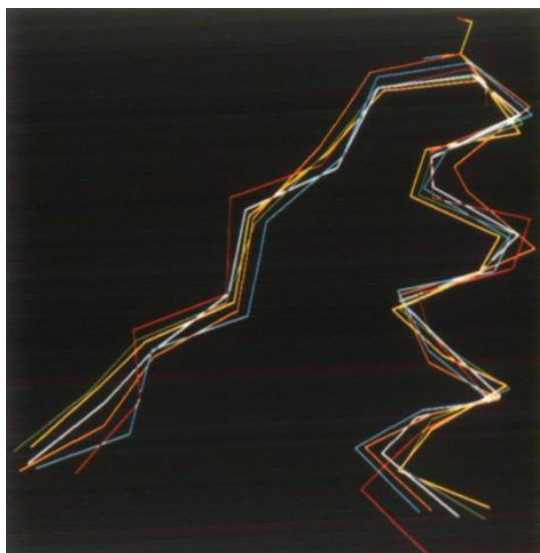


Figure 2: Figure: A Ca diagram of the nucleophile elbow of the α/β hydrolase fold enzymes. Shown are Acetylcholinesterase(AChE) - green, wheat carboxypeptidase II (CPW) -orange, diene lactone hydrolase (DLH) -white, haloalkane dehalogenase (HAL) - red, Lipase (GLP -yellow) and triacyl glycerol lipase (MLIP) – blue (Ollis et al. 1992).

Enzymes that belong to this family often have a molecular mass between 25-65 kDa. They can operate on substrates with completely different chemical or physicochemical properties. Most of these enzymes do not require any co-factors for their function (Damborsky and Koca 1999; Fetzner and Steiner 2010; Steiner et al. 2010); whereas other enzymes with this architecture require metal ions for the enhancing stability (Tyndall et al. 2002; O'Connor & Stockley 1986). The α/β hydrolase fold family includes proteases, lipases, esterases, dehalogenases, peroxidases and epoxide hydrolases, making it one of the most versatile and widespread protein folds known (Nardini and Bauke 1999).

1.2.1. Cutinases

Cutinases or cutin hydrolases [EC 3.1.1.74] are enzymes originally discovered in phytopathogenic fungi which use cutin as carbon source. They have a molecular weight around 22,000 daltons (Carvalho, Aires-Barros, and Cabral 1998) with highly conserved stretches, which include four invariant cysteines, forming two disulfide bridges. The Cutin is integrated and over-layered by intracuticular and epicuticular waxes, complex mixtures of hydrophobic material containing very long-chain fatty acids and their derivatives. The combination of cutin, waxes and possibly polysaccharides, forms the cuticle (Jeffree 1996) Since their discovery in the early 1970s, various fungal and bacterial cutinases have been purified and characterized. Their role regarding the penetration of intact plant surfaces is well documented (Kolattukudy 1985; Purdy and Kolattukudy 1975). These properties can be even used to

enhance the pharmacological effect of chemicals used in agriculture (Genencor 1988). Figure 3 shows a simplified drawing of the plant cuticle

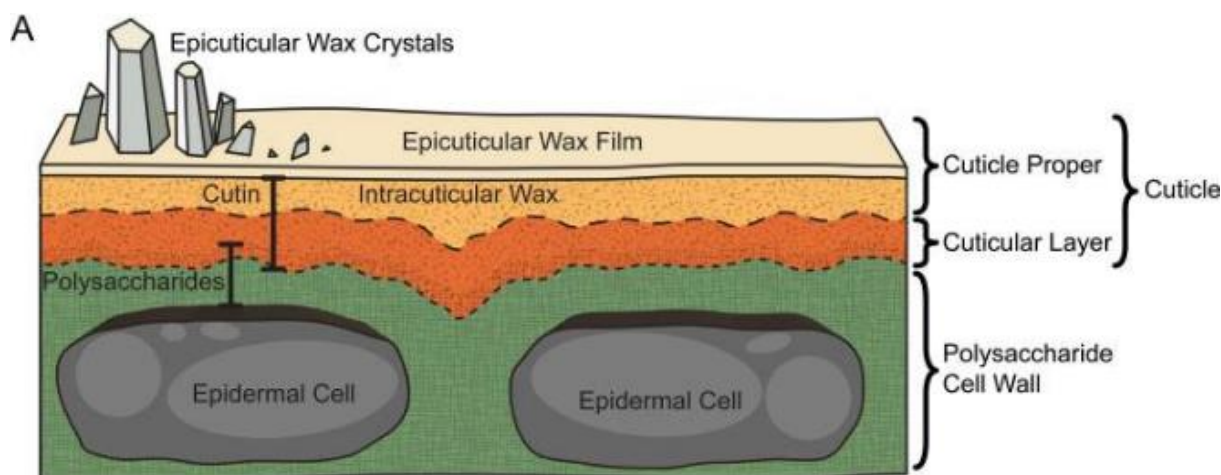


Figure 3:A schematic drawing of the plant cell wall/cuticle complex of focusing on the main structural parts. (Yeats and Rose 2013)

Cutinases combine catalytic properties of lipases and esterases, therefore show catalytic activity in water, as well as in oil interfaces. A big difference to lipases is the absence of interfacial activation, meaning the ability to shield the active site from the solvent which gets accessible in the presence of a lipid/water interface (Carvalho et al. 1998; Grochulski et al. 1993). Their lipolytic ability makes them useful for many industrial applications such as hydrolysis of triglycerides and esters (Flipsen et al. 1996; Gonçalves, Cabral, and Aires-Barros 1996), esterification (Sebastião, Cabral, and Aires-Barros 1993) or as laundry or dish water agent for the removal of fats (Flipsen et al. 1998; Okkels 1997; Unilever 1994). In addition, their high or even amplified stability in organic solvents (de Barros et al. 2011) and ionic liquids qualify cutinases together with lipases and esterases for application in industrial processes with challenging process conditions (Klähn, Lim, and Wu 2011). In non-aqueous environments this enzyme can be used for synthesis of short chain aliphatic esters (Abo, Christensen, and Hu 2011; Nikolaivits, Makris, and Topakas 2017; Su et al. 2016) to polyesters (Alessandro Pellis, Herrero Acero, et al. 2016; Pellis et al. 2017). Together with other hydrolases, these enzymes are often employed in organic chemistry, due to their wide availability, low cost as well as substrate specificity and independence from cofactors.

In terms of plastic degradation, Cutinases from *Thermobifida fusca* (Thf42_Cut1) and *Thermobifida cellulolysitica* (Thc_Cut1 and Thc_Cut2) were characterized regarding PET hydrolysis and compared to structurally related cutinases to evaluate their hydrolysis activity (Gomes et al. 2013).

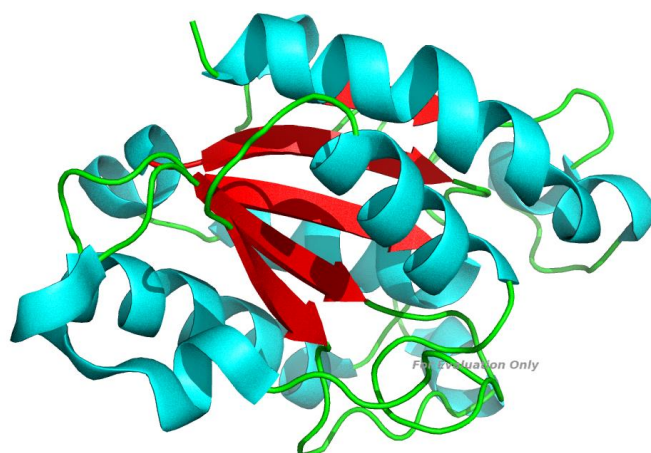


Figure 4: Cartoon model of *Humicola insolens* cutinase (Own image created with PyMol® software)

1.3. Green chemistry

The essential tasks of sustainable development are reducing the negative environmental impact of the substances that we use and generate. Therefore, a fundamental change towards renewable energy production und substitution of oil based chemicals is necessary. Although it is not possible to predict the exact date of exhaustion of fossil fuels its most likely that it the majority or oil-, gas-, and coal reserves will be depleted by 2100 (Höök, Sivertsson, and Aleklett 2010)

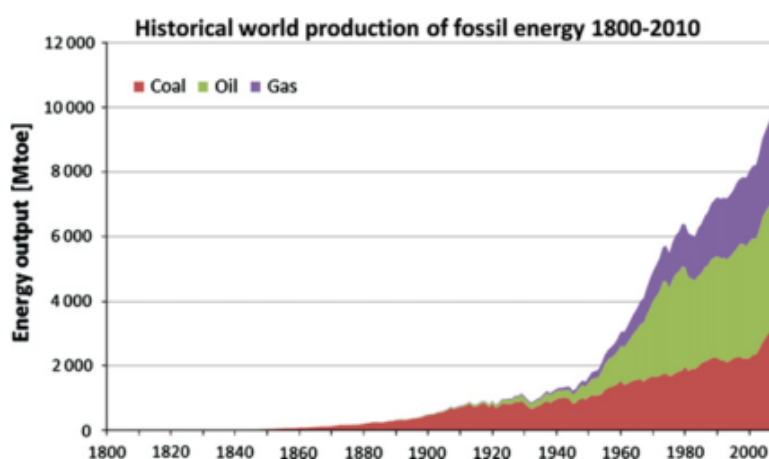


Figure 5: Global production of fossil energy from 1800 to 2010 (Höök et al. 2012)

Since the 1990s, certain trends regarding environmental friendly processes have established. Notable achievements have been made for example in application of supercritical fluids for chemical reactions

(Brunner 2004). While it is difficult to give an exact definition for green chemistry, 12 aims and principles, established by the American Chemical Society such as use of safer and less toxic chemicals and solvents, atom economy (maximize incorporation of all materials used in the process), design for energy efficiency, use of renewable feedstocks, reduction on derivatives among others define the outline of this term (Anastas and Warner 1998). Modern approaches such as continuous flow processes (Wiles et al. 2014) can help to establish sustainable and efficient production of chemicals, where operation under pressure enables use of low boiling solvents and reagents at elevated temperatures. Precise reaction control and cost reduction among other advantages come with these new techniques.

1.4. Poly ethylene terephthalate

Poly(ethylene terephthalate) is one of the most important polymers today. It is a thermoplastic polymer with high tensile and impact strength, transparency and sufficient thermal stability (Zimmermann and Billig 2010) and wide variety of applications. The crystallinity grade can vary from high amorphous to high crystalline. Except for alkaline or acidic treatment, it shows a high chemical resistance (Goodfellow Inc. 2003). Polyethylene terephthalate can be produced in two ways:

The dimethyl terephthalate process shown in Figure 6 is performed in two synthesis steps with the name giving compound and excess ethylene glycol starting 150–200 °C with a basic catalyst. Methanol (CH₃OH) needs to be removed by distillation to drive the reaction forward. Excess ethylene glycol is distilled off at higher temperature with the aid of vacuum. The second transesterification step proceeds at 270–280 °C, again with continuous removal of ethylene glycol as well. (Köpnick et al. 2000).

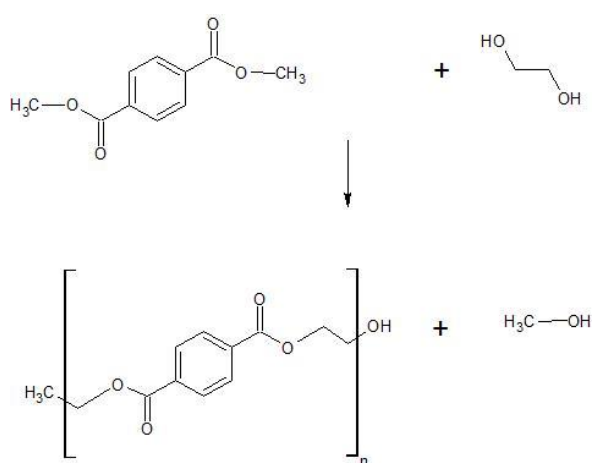


Figure 6: Synthesis of PET using the dimethyl terephthalate process

The terephthalic acid process is achieved directly at moderate pressure (2.7–5.5 bar) and high temperature (220–260 °C) (Köpnick et al. 2000). The reaction is shown in Figure 7.

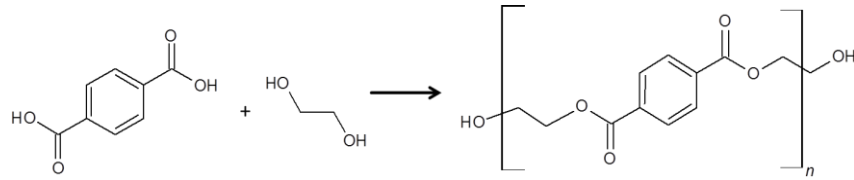


Figure 7: Synthesis of PET using the terephthalic acid process

For polymerization, purified terephthalic acid (pTA) and mono ethylene glycol (MEG) are the preferred precursors for synthesis of PET since Water is the only byproduct (Pang, Kotek, and Tonelli 2006). Figure 8 gives a simplified overview on the complete process chain. This synthetic polymer can be found in different applications: fabrics, bottles, films or engineering plastics (Ji 2013).

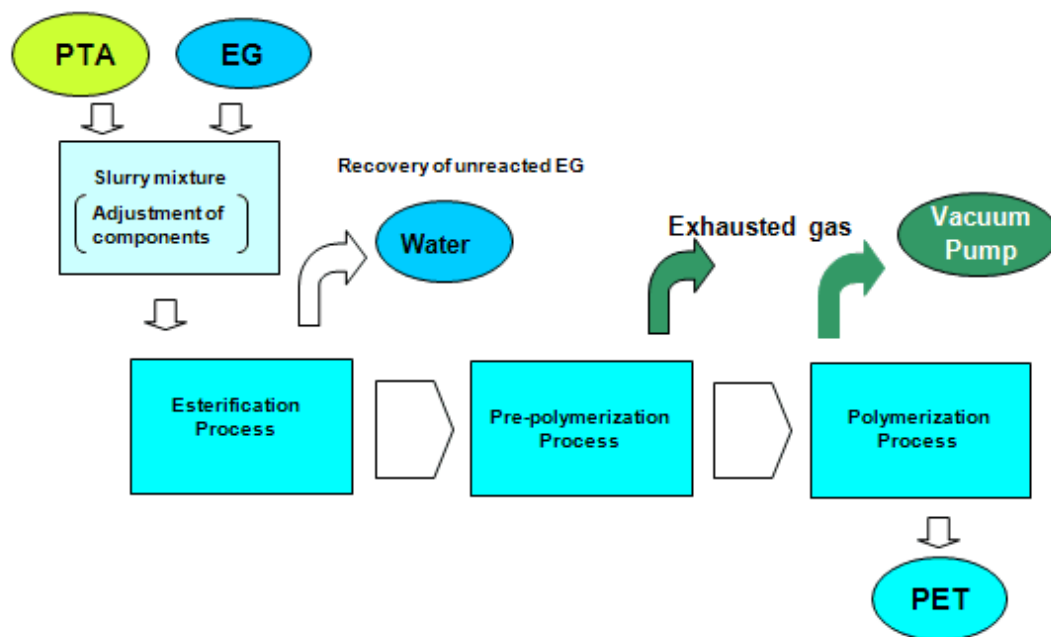


Figure 8: Process scheme PET production (HITACHI 1994)

1.4.1. Application of PET for synthetic fiber production

The textile and clothing industry covers different types of fibers, with about 54% synthetic materials. The consumption of these synthetic fibers increased between 2000 and 2012 by 77% (Harder et al.

2014). As a consequence, the increase of synthetic fibers in global consumption results in the rising demand for petroleum-based chemicals (Alessandro Pellis, Herrero Acero, et al. 2016).

Regarding the textile industry, Two PET grades are dominating the global market: the fiber grade PET, with a MW of 15-20 kg*mol⁻¹ and intrinsic viscosity between 0.4 and 0.75 dL*g⁻¹ and the bottle grade PET, which refers to a higher MW polymer (>20 kg*mol⁻¹) with an intrinsic viscosity above 0.95 dL*g⁻¹ (Al-Sabagh et al. 2016; Tasca et al. 2010)

In the year 2010, the World fiber production has been exceeding 64 million tons per year (Wang 2010). Extensive energy consumption during is necessary during the complex production processes (Kocabas et al. 2009). Figure 9 shows the composition of textile products. Blends represent a rather large fraction (42%) since special characteristics like wettability, elasticity or appearance can be altered by combining different materials in specific ratios. Additionally, the production process can become more cost efficient due to improved spinning.

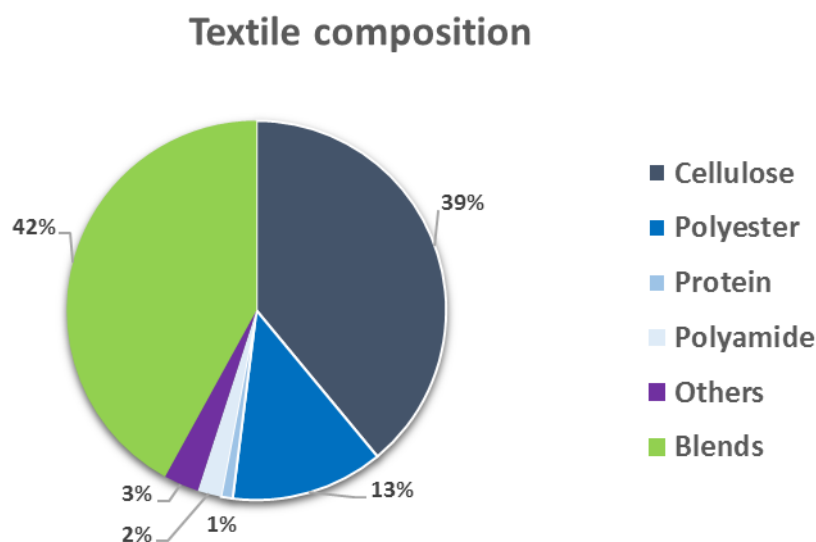


Figure 9: Used textile composition (Own diagram, data from SOEXGroup (Germany))

Due its wide production and utilization (Guebitz and Cavaco-Paulo 2008), PET represents a broad disposal inert textile. The non-toxic nature, durability and crystal-clear transparency of PET during use are the principal advantages of this polyester, while its rather slow biodegradability is the major cause of concern to the environmentalists. Recycling the textile waste-derived polyesters can significantly cut down the energy usage, resource depletion and greenhouse gas emissions.

1.4.2. Chemical and Mechanical recycling

Several approaches exist to reduce the overall amount of plastic waste and pollution with plastic residues. Unfortunately, different factors such as coloring dyes (Giannotta et al. 1994) and other

chemicals such as detergents, fuels and pesticides (Demertzis et al. 1997), reduce the quality of recycled PET and its possible applications. Energy efficient removal of dyes can be achieved with cellulases, hemicellulases or laccases (Ibarra et al. 2012)

Recycling on a chemical basis can be separated in alkaline/acid hydrolysis, or substrate specific hydrolysis, namely glycolysis, methanolysis and other processes like aminolysis and ammonolysis (Sinha, Patel, and Patel 2010). The most suitable option for degradation of PET is alkaline hydrolysis using 4–20% NaOH/KOH solutions (Karayannidis, Chatziavgoustis, and Achilias 2002) and acidic hydrolysis using concentrated sulphuric acid or other mineral acids (Toshiaki Yoshioka, Tsutomu Motoki, and Okuwaki 2000). Mechanical recycling has the aim to mechanically separate the polymer from contaminants so it can be directly reprocessed to granules via melt extrusion (Sinha et al. 2010).

1.4.3. Other recycling techniques

Recent advances have been made to accelerate biodegradation (Mueller 2006) or modify the surface of PET by various methods like activation of PET substrate for functionalization with an organic catalysts like TiO₂ (Webb et al. 2012). In the last decade, the interests of sustainable technologies targeting polyester biodegradation and recycling are gaining a key role. Yoshida et al. showed a novel bacterium, *Ideonella sakaiensis* 201-F6, able to break down PET films using two enzymes for hydrolysis and assimilation of its building blocks for growth (Yoshida et al. 2016). Earlier, various studies demonstrated that a class of enzymes belonging to the α/β hydrolase family, namely cutinases, are able to hydrolyze the ester bonds of PET and several other polyesters (Pellis et al. 2016; Pellis et al. 2015; Wei et al. 2016; Barth et al. 2016). Among them, cutinases are currently under investigation for the bioprocessing of PET textiles on an industrial scale (Silva et al. 2005). Earlier, it was reported that cutinases from *Thermobifida fusca* and *Humicola insolens* were able to hydrolyze low crystallinity PET while complete hydrolysis by enzymes only seems to be difficult if not impossible for PET with higher crystallinity (Mueller 2006; Nimchua, Punnapayak, and Zimmermann 2007; Ronkvist et al. 2009). Furthermore, it has been performed a synergistic chemo-enzymatic hydrolysis of PET able to produce high purity TA avoiding harsh chemical treatment (Quartinello et al. 2017).

1.5. The RESYNTEX project

This project aims to integrate a holistic approach regarding waste textile recycling for creating a circular economy concept focusing on textile and chemical industries. Better REcycling shall provide new secondary raw materials. Various fields are combined through SYNthesis and TEXtiles are transformed into chemical feedstock for synthesis of new goods.

The output after processing of the starting material using a combination of chemical and biotechnological decomposition strategies, should serve as secondary raw materials to produce new

polymers. 20 project partners from 10 different EU countries contribute to this project. Besides reduction of textile industry based environmental impact, new chemical feedstock material at reasonable costs, increased public awareness and recycle options are the desired outputs.

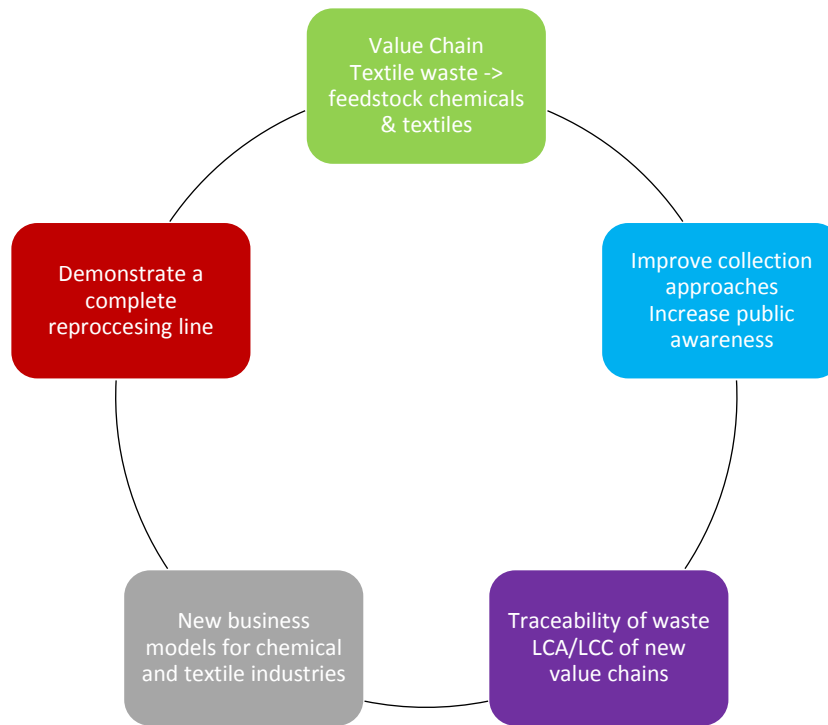


Figure 10: Core goals of the Resyntex project (Resyntex 2017)

Figure 10 gives a “simplified overview” on the core goals of the project. Figure 11 shows a more detailed processing scheme where the complete transformation from waste to economically relevant products and chemical feedstocks is visualized.

Table 2 gives a short description of each work package.

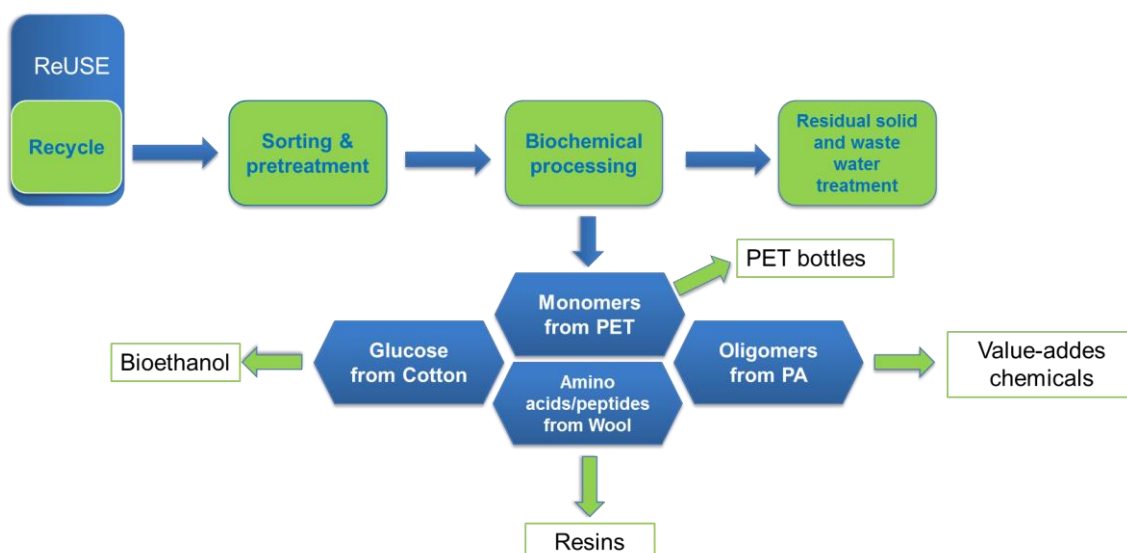


Figure 11: Processing steps from waste material to chemical feedstock and value added products (Resyntex 2017)

Table 2: The Resyntex work packages (Resyntex 2017)

Work package 1	Design of a complete value chain beginning with textile waste collection through to the generation of new feedstock for chemicals and textiles
Work package 2	Improvement of waste collection approaches, particularly for non-wearable textiles, by encouraging behavioral change. Analysis of stake holders, promotion of recycling and focus on increasing social awareness and involvement are also part of this package.
Work package 3	Development of a process for transforming textile waste into a suitable feedstock for recycling. The process must be suitable for mechanical production line, sorting multicomponent waste and general preparation for recycling
Work package 4	For the transformation of natural fibers, such as cotton and wool, as well as synthetic fibers, an environmentally-friendly process into feedstock intermediates outlined. The combination of chemical and enzymatic treatment enables enhanced decomposition while keeping energy costs low compared to full chemical hydrolysis
Work package 5	Aims to develop industrial applications for the recovered feedstock from work package 4. Activities will involve end-users and experts, allowing effective exploitation of feedstock.
Work package 6	This will produce process designs and flow sheets for Resyntex at full scale. It will address all recovery stages needed for a single plant
Work package 7	The Resyntex concept will be tested in an industrial environment. Development of a demo-scale environment

Work package 8	The established textile waste recycling value chains will be evaluated regarding its performance via life cycle assessment (LCA) and life cycle costing (LCC)
Work package 9	Communication and Dissemination
Work package 10	Project management

1.5.1. Work package 4

The WP 4 can be separated in to recovery of recovery of wool, cellulosic fiber discoloration and recovery as well as PET and PA recovery. Different enzymes and preprocessing strategies need to be applied for each fiber material.

Process Flow Diagram: New Proposal

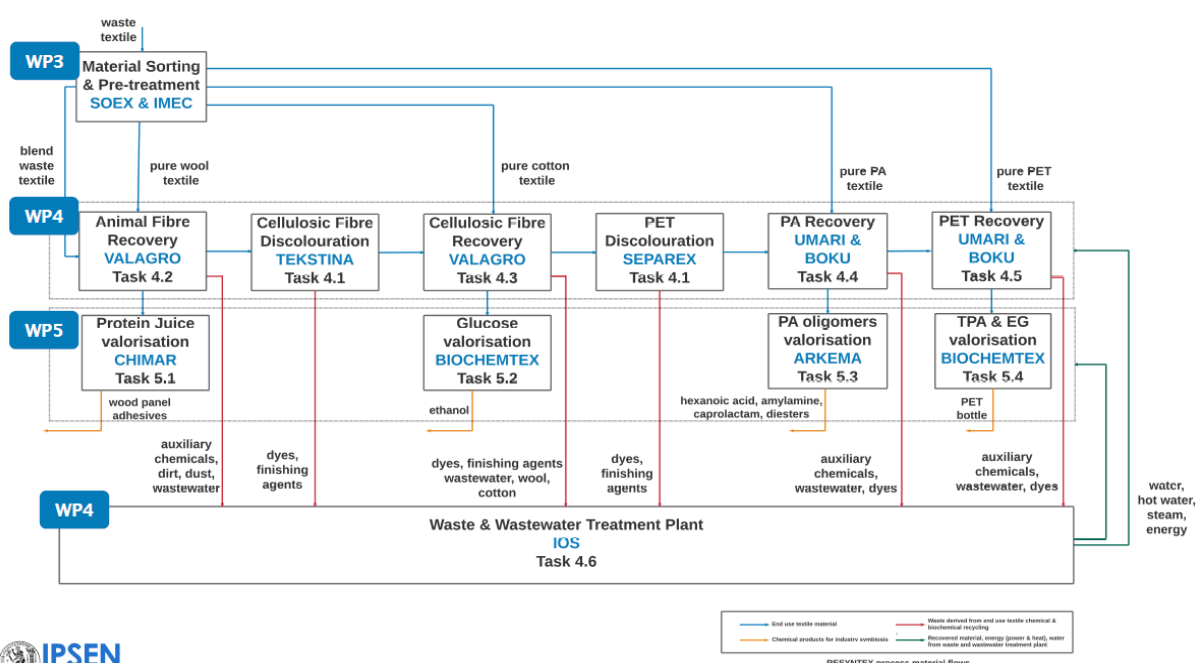


Figure 12: Detailed process scheme of Work package 4 (Resyntex 2017)

1.6.Immobilization of enzymes

Enzymes catalyze the reaction both in free form in solution and immobilized on a support. The free enzyme has a very short stability and the recovery is difficult after its use in the reaction mixture. The use of free enzyme requires many cycles of expression and purification, which is an important economic factor in industry. In addition, immobilization makes it easier to reuse the catalysts and therefore increase its productivity. Another important factor is the increased stability and storage and operational conditions. Immobilization of enzyme inside a porous structure protect the enzyme against aggregation

autolysis or proteolysis that might occur in the reaction solvent (Mateo et al. 2007) Contact with hydrophobic surfaces such as air bubbles that could lead to inactivation (Bommarius and Karau 2005; Caussette et al. 1998) is avoided as well.

Therefore, besides others, several strategies have been developed to enable the immobilization of the enzymes.

Enzymes are defined “immobilized” when confined in a region of a support, while retaining their catalytic activity (Brena and Batista-Viera 2006). Once immobilized, the enzyme can be easily separated from the reaction products and reused for several times. Possible applications have been reported for various fields (Kallenberg, van Rantwijk, and Sheldon 2005; Kirk, Borchert, and Fuglsang 2002; Soumanou and Bornscheuer 2003; Würtz Christensen et al. 2003). A negative factor of immobilization is the reduction of the catalytic activity, due the fact the enzyme can be immobilized with different orientations, reducing the accessibility to the substrate and reducing motion for the dynamics. The carrier also becomes “useless” when an irreversibly bound enzyme loses its activity.

1.6.1. Carrier bound immobilization

The choice of support and linker has a great influence whether a reduction of substrate accessibility and therefore loss of activity can take place. The support should be inert for reducing the inhibition of the enzyme, but the groups on the surface could be formed for specific immobilization. Typical materials are synthetic resin, bio- polymer or inorganic polymers such as (mesoporous) silica or a zeolite. Environmentally friendly materials became more popular as carrier material over the last years (Datta, Christena, and Rajaram 2013). A summary of carrier bound immobilization strategies and functional groups is presented by Cantone (Cantone et al. 2013).

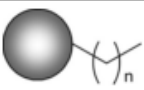
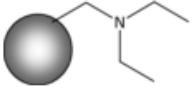
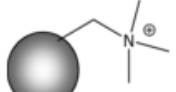
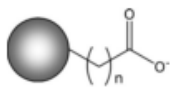
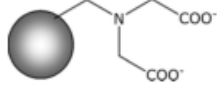
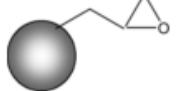
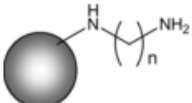
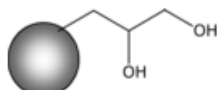
Method of immobilisation	Functional group	Structure	Binding	Reactive group on enzyme
van der Waals and hydrophobic interactions	Alkyl		The long alkyl chain enhances the hydrophobic nature of the carrier and maximizes hydrophobic interactions for physical immobilisation (adsorption)	Hydrophobic areas on the surface of lipases
Ionic interactions	Trialkyl ammine		Ionic adsorption	Negatively charged a.a.
	Tetra alkyl ammonium		Ionic adsorption	Negatively charged a.a.
	Carboxylate		Ionic adsorption	Positively charged a.a.
Metal affinity	Iminodiacetic		Loading metals such as Ni ²⁺ , Zn ²⁺ , Cu ²⁺	His-tag
Covalent bonds	Epoxy		Formation of covalent bonds <i>via</i> nucleophilic attack and opening of the epoxy ring	Nucleophilic groups (mainly -NH ₂ and -SH)
	Amino		Pre-activation with glutaraldehyde to introduce an aldehyde group that forms an imino bond <i>via</i> nucleophilic attack by a primary amine	Primary amines (terminal amines and Lys side chains)
	Diol		Activation with BrCN to give a reactive cyclic imido-carbonate Oxidation of adjacent <i>cis</i> -diols with NaIO ₄ to give dialdehydes	Primary amines (terminal amines and Lys side chains)

Figure 13: Techniques for carrier bound immobilization (Cantone et al. 2013)

The methods of linkage between the enzyme to enzyme or enzyme to support are divided in two classes:

- **Irreversible immobilization:** The enzyme cannot be detached from the support without destroying the structure of the biocatalyst. These types of immobilization are based on the formation of covalent bonds or with entrapment techniques. Coupling can be performed with the activation of matrices or modification of the polymer backbone to produce active groups whereas entrapment techniques is based on the occlusion of the enzyme inside a polymer network, where substrates and products can pass through but the enzyme could not.
- **Reversible immobilization:** In this case the biocatalyst is bound to the support under gentle conditions. Usually are involved adsorption, van der Waals forces, hydrophobic interactions and chelation binding.

The reasons why immobilization via epoxy linker is most suited for HiC is the simple immobilization protocol, due to high stability at neutral pH even under wet conditions and lack of drawbacks as found in other immobilization protocols (Cesar Mateo et al. 2000) and the fact that the epoxy linker binds to lysine residues which in this case, are far away from active site ensuring a sufficient accessibility (Figure 14).

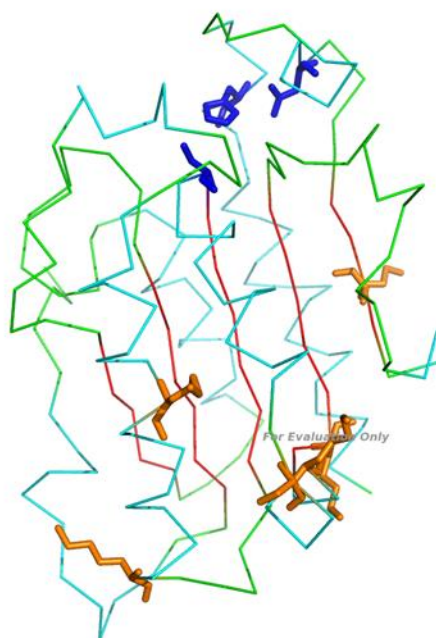


Figure 14: Stick Model of *Humicola insolens* Cutinase (Own image created with PyMol® software) with highlighted lysines (orange sticks) and the active site (in blue: Serine 105, Histidine 173 and aspartic acid 160 (Kold et al. 2014))

1.6.2. Entrapment

Via inclusion of the enzyme in a polymeric network consisting of organic polymers, silica sol-gel, hollow fiber or micro capsule, indirect immobilization takes place. The binding forces are too weak to prevent 100% leakage (Sheldon 2007), therefore, additional covalent attachment is often required. The polymeric network needs to be synthesized in the presence of a catalyst showed for the first time in silica sol gels by Braun and Co-Workers (Braun et al. 1990). This method was later improved and is now a widely used form of enzyme entrapment (Reetz 1997). Newer approaches focus on sustainable, biobased materials like Gelatin in combination with encapsulation techniques (Shen et al. 2011) or hydrogel based entrapment (Mariani, Natoli, and Kofinas 2013).

1.6.3. Cross-linking

Previous discussed carrier based techniques might lead to lower space time yields and productivities as a consequence of the large fraction of non-catalytic material (Tischer and Kascher 1999). Hence a rising

interest for cross-linked enzyme crystals (CLECs) and cross-linked enzyme aggregates (CLEAs) was developed. CLECs were commercialized in the 1990s by Altus Biologics. Advantages are highly concentrated enzyme activity, high stability and low production costs, since additional carrier material is obsolete. applicable to a broad range of enzymes CLECs are significantly more resistant to heat, organic solvents and proteolysis than the corresponding soluble enzyme or lyophilized (freeze-dried) powder. CLECs are robust, highly active immobilized enzymes of defined particle diameter, varying from 1 to 100 μm . CLEAs are created via addition of salts, water-miscible, organic solvents or non-ionic polymers, to aqueous solutions (Sheldon 2007).

2. Materials

2.1. Buffers

Hydrochloric acid	Sigma-Aldrich (USA)
Tris(hydroxymethyl)-aminomethan (Tris)	Sigma-Aldrich (USA)
HAc	Merck (Germany)
NaAc	Sigma-Aldrich (USA)
NaOH	Sigma-Aldrich (USA)
KH ₂ PO ₄	Sigma-Aldrich (USA)

2.2. SDS-PAGE

SDS chamber	Biorad (USA)
SDS gels	Biorad (USA)
PageRuler™ Prestained Protein Ladder, 10-180 kDa	Thermo Fisher Scientific (USA)
SDS PAGE 4x Samplebuffer	Biorad (USA)
β-Mercaptoethanol	Merck (Germany)
Coomassie Brilliant Blue R250	Sigma-Aldrich (USA)

2.3. Immobilization

<i>Humicola Insolens</i> cutinase (HiC)	Novozymes (Denmark)
SEPABEADS™ EC-EP/M	Resindion (Italy)

2.4. Determination of protein concentration

Bovine Serum Albumin	Sigma-Aldrich (USA)
Bio-Rad protein assay 5x Solution	Bio-Rad (USA)

2.5. Determination of enzyme activity

<i>p</i> -NPB	Sigma-Aldrich (USA)
HCl	Sigma-Aldrich (USA)
Tris(hydroxymethyl)-aminomethane	Sigma-Aldrich (USA)

2.6. Analysis of Substrate and Monomers

Terephthalic Acid	Fluka (USA)
BHET	Fluka (USA)
3PET	Clariant (Switzerland)
PET	Clariant (Switzerland)
Methanol	ROTH (Germany)
Formic Acid	Sigma-Aldrich (Germany)
Resyntex sample: EE21A ¹	University of Maribor
Resyntex sample E21A (EE21A before lyophilization)	University of Maribor
Resyntex sample EE21B	University of Maribor
Resyntex sample EE21C	University of Maribor

¹ Sample description is section 3.6.5

3. Methods

3.1. Bradford assay

The Bradford assay was performed to monitor the state of immobilization as well as possible leaching as a consequence of the incubation conditions. Before each measurement, a standard calibration with Bovine Serum albumin (BSA) was performed. (Appendix)

- 10 µL of the sample was added in to each well of a 96 well plate, followed by 200 µL of prepared BioRad reaction solution (BioRad reagent diluted 1:5 with MQ water).
- The plate was then incubated at 400 rpm for 5 min at room temperature. The buffer for protein solution is used as a blank (Tris/HCl, 0.1 M, pH 7.0). In case of the standard calibration, P-Ki 0.1 M, pH 7.0 was used as a blank.
- Absorption after 5 minutes was measured at 595 nm.

.

Calibration:

$$y = k * x + d \quad (1)$$

y...Absorbance

k...slope of regression line

x...concentration of analyte

d...intercept

3.2. SDS- PAGE

- The samples were mixed 1:1 with 2x Laemmli buffer (for composition see Appendix). For dilutions MQ-H₂O was used. After mixing, the samples were denaturated at 100 ° for 5 min.
- The loading volume for samples was 12 µL, For the protein marker (PageRuler™), only 5 µL were used. The total running time was 45 min, (Voltage 160 V.) After the run, the gel was stained for 45 min in Coomassie brilliant blue R250 staining solution and destained for 1 hour with destaining solution (two times).

3.3. Fourier Transform Infrared(FT-IR) spectroscopy

The samples from the university of Maribor were characterized using a Perkin Elmer Spectrum 100 FT-IR Spectrometer according to Quartinello *et al.* (Quartinello et al. 2017). Spectra were collected at a resolution of 4 cm⁻¹ for 15 scans. In parallel the spectra of pure PET and pure PA were recorded as described above

The bands were assigned as follows: 3600 – 3100 cm⁻¹ν(NH₂), 3600 – 2900 cm⁻¹ν(OH), 2996-2945 cm⁻¹ν(CH₂) and ν(CH₃), 1748 cm⁻¹ν(CO), single band 1620 cm⁻¹ δ(NH₂), single band 1590 cm⁻¹ν(CC), 1452 cm⁻¹ δ(CH₂), 1299 cm⁻¹ν(CO-C), 1128 cm⁻¹ν(CO), 957 cm⁻¹ν(CO-C).

3.4. *para*-(Nitrophenyl substrate) activity assay

3.4.1. Activity of free enzyme

- An aliquote of pure *p*-NPB stored at -20°C was put on ice to thaw slowly.
- 86 µL of the aliquote were mixed with 1 mL of ice cold 2-methyl-2-butanol. The substrate solution was covered with aluminum foil.
- From this solution 120 µL where mixed with 3 mL of buffer (Tris/HCl 0.1 M, pH 7/8.5; K-Pi 0.1 M, pH 7; NaAc 0.1 M, pH 5.5)
- The solution was stored in a 15 mL falcon tube, covered with aluminum foil and stored on ice (reaction solution).
- 20 µL of enzyme samples were put in each well of a 96 well plate. Maximum 12 well or 4 samples in triplicates were measured at a time. 200µL of the reaction solution was added to the previously filled wells und measured immediately.
- The absorption at 405 nm was measured for 5 min in cycles of 18 sec. Reaction temperature was 30 °C.

Activity - free enzyme:

$$A = k * \frac{V_{\text{total}}}{V_{\text{sample}} * \epsilon * d} * f \quad (2)$$

A...	Activity	U*mL ⁻¹
k...	Slope	Abs*min
V _{total}	Total volume	mL
V _{sample}	Sample volume	mL

ϵ	Molar extinction coefficient of <i>p</i> -NPB at 405 nm 9.36 (pH: 7) 16.67 (pH: 8.5)	$\text{mL}*(\mu\text{Mol*cm})^{-1}$
d	Well thickness	cm
f	Dilution factor	

3.4.2. Activity of immobilized enzyme

- 20 mg of immobilized HiC were mixed with 11 mL of Tris/HCl 0.1M, pH 7 +100 μL *p*-NPB substrate solution (86 μL stock + 1 mL 2-methyl-2-butanol).
- Activity was measured at 23°C, incubation was performed at 100 rpm, 30 °C. The activity of the same sample was measured at 3, 6, 9, 12, 15 min. Samples were measured in duplicates. In addition, two blanks, only filled with buffer, unused beads and substrate solution where measured as well.
- The dilution of samples was performed in the glass cuvette. The dilutions were prepared in advance. Absorbance was measured at 405 nm

Sample	0 min	3 min	6 min	9 min	12 min	15 min	18 min
Dilution	1:4	1:6	1:6	1:6	1:6	1:6	1:6

Activity

imm Enzyme [U/g_{dry}]

$$A = (Abs_x * d - Abs_{Bl} * 3) * \frac{11.1}{8.2 * t * m_{Beads}} \quad (3)$$

A...	Activity	$\text{U}*\text{g}^{-1}$
Abs _x	Absorption of the sample	
d...	Dilution factor	
Abs _{Bl}	Absorption of the blank	
t	Incubation time	min
m _{Beads}	Mass of Beads	g

3.5. Immobilization

- For immobilization of *Humicola insolens* cutinase, 5g of SEPABEADS™ EC-EP/M beads were weight and stored for later use.

- The initial concentration of the enzyme stock solution was 11.21 mg/mL. 4.5 mL of aliquoted stock solution were put in to a 50 mL falcon tube. The tubes with the aliquots were rinsed with 600-800 μ L Tris/HCl 0.1 M, pH 7. The rinsing solution was then added to the falcon tube and further filled up to 40 mL to obtain a final concentration of 1.25 mg/ml.
- 300 μ L of the diluted enzyme solution stored at -20°C. More tubes where prepared for taking samples after 1, 2, 3, 5, 6, 7, 8 hours after the start immobilization reaction.
- After adding the beads to the enzyme solution, the falcon tube was placed on a rotation wheel at a rotating speed of 60 rpm. The reaction was performed at room temperature.
- The samples at each time point were frozen at -20 °C and stored together with the initial sample at time point zero (t_0).
- On the next day, a sample was taken after 24 hours reaction time. The mixture was filtered through a paper filter. The beads were washed 3 times with 30 ml fresh buffer and left in the filter to dry for 24h. The filter was placed in a desiccator and dried further for another 48 hours.
- The frozen samples were analyzed *via* Bradford assay and *p*-NPB activity assay to determine the residual concentration of enzyme in the supernatant and further to obtain the immobilization efficiency.

Immobilization efficiency:

$$I_{\text{eff}} = \frac{c_{t_0} - c_t}{c_{t_0}} * 100\% \quad (4)$$

I_{eff} Immobilization efficiency [%]

c_{t_0} Protein concentration at t_0 [mg/mL]

c_t Protein concentration at t [mg/mL]

3.6. Optimization of reaction conditions

Each set of experiment was diluted with 3 mL of buffer, an equivalent amount of free HiC was used in the same amount of buffer in order to compare effects of changed reaction conditions to both types of enzymes. Therefore, the protein concentration of the stock solution was determined every two weeks and the amount of added stock solution to the sample vessel adapted. The equivalent volume of the enzyme stock solution was directly added to 3 mL of buffer.

weight iHiC:

$$m_{\text{iHiC}} = m(\text{Beads}) * 1\% \frac{m(\text{HiC})}{m(\text{Carrier})} * I_{\text{eff}} \quad (5)$$

specific
Hydrolysis
rate iHiC

$$A_{\text{PET}}(\text{iHiC}) = \frac{c(\text{Monomer}) * f * V_{\text{sample}}}{\frac{m_{\text{iHiC}}}{M_r(\text{iHiC})}} \quad (6)$$

3.6.1. Long time stability

- 40 mg iHiC were put in to 30 mL glass vials and incubated at 50°C and 100 rpm. The vessel was filled up to 11 mL with Tris/HCl 0.1M, pH 7. To obtain better mixing conditions, the samples were incubated vertically. All samples were prepared in duplicates. The incubation was stopped after 1, 3, 5, 8, 24, 48, 72, 168 and 672 hours. After the desired incubation time, the samples were stored at 4°C for further use.
 - 1mL was taken from each sample to determine concentration and activity of leached enzyme. Reactions with the substrate (PET powder, 8% crystallinity) were always performed for 69 hours (initial reaction time with substrate under same conditions. The second reaction was performed with all samples at once. For comparison, a fresh sample of iHiC was used as well to compare the storage conditions: dry storage 21°C. Storage in buffer at 4°C.
 - The supernatant of the samples t₀-t₈ was checked for protein concentration and activity.
 - The supernatant of t₂₄-t₆₇₂ was only checked for protein concentration
 - Before incubation with PET powder, the remaining buffer was removed with a glass pipette and all samples were further dried at 55°C for 45 min. 11 mL fresh Tris/HCl buffer was added to each well
 - All samples were incubated for another 69h under same reaction conditions
 - Variation of experimental conditions:
 - Incubation vertical/horizontal
 - Shaking conditions varied between 100 and 190 rpm
- Reduction of reaction volume:
20 mg of iHiC was combined with 5 mg of PET powder. 1.5 mL of buffer (Tris/HCl 0.1 M, pH 7) was added.
- Incubation time was 120h. Samples were taken with a frequency of 24h.

3.6.2. Washing stability

- The Weight of the loaded beads was noted, then the samples were washed for 0, 5 and 10 times. As washing solution 5 mL of Tris/HCl 0.1M, pH 7 was used. After adding of the solution. The vessel was incubated at 350 rpm at room temperature for 1 min. 100 µL of the supernatant was taken for analysis with Bradford and *p*-NPB activity assay.
- To see a possible influence of the pH, the same experiment has been performed with Tris/HCl 0.1 M, pH 8.5 and NaAc 0.1 M, pH 5.5.

3.6.3. pH stability

- For checking the influence of the pH on hydrolysis, the samples were incubated at different pH levels at 50°C and 70°C and 100 rpm.
- For all samples blanks with PET/buffer, pure buffer as well as Bead/PET/Buffer were prepared. The following Buffers have been used:
 - Tris/HCl 0.1 M, pH 8.5
 - K-Pi 0.1 M, pH 7
 - NaAc 0.1M, pH 5.5 NaAc 0.1M, 4.6
 - NaAc 0.1M, pH 3.6
- 40 mg of iHiC was weighed in to a 30 mL glass vial with 10 mg of PET powder and 11 mL of buffer. The sample was incubated in upright position at 50°C, 190 rpm for 24 h and further incubated until 69h to make it comparable to the stability experiment.
- 40 mg of iHiC and 10 mg of PET powder were weighed into 5 mL tubes. 3 mL of buffer was added to each tube. The samples were incubated at 100 rpm, 50°C. All samples were prepared in triplicates.
- The samples were incubated in horizontal position at 50°C, 100 rpm for 5 days or 120h. After 24, 48, 72, 96 and 120h 500 µL were removed for analysis with *p*-NPB activity and Bradford essays. Samples with the same amount of fHiC were incubated under same conditions. All samples were prepared in triplicates.

3.6.4. Influence of shaking

- 20 mg of iHiC was added to 2 mL tube and mixed with 5 mg of PET powder. A volume of 1.5 mL of buffer was added and the tube sealed with parafilm. Incubation conditions were 50°C, 0 rpm 120h.
- In total 15 samples of iHiC and 15 samples of fHiC were prepared. With a frequency of 24h these samples were removed from the incubator to stop the reaction.

3.6.5. Incubation with chemically preprocessed substrates

Water based PET hydrolysis was performed in a 1 L stainless steel reactor suitable for high pressure and high temperature at 250 °C and 39 bar to achieve depolymerization of the sample (Quartinello et al. 2017). All experiments were carried out with 12,5 g of virgin PET fiber +12,5 virgin PA in 250 mL

deionized water (ratio substrate/water 1:10). The reaction was stopped after 60 min. This led to a degradation of the substrate into a whitish powder which was then analyzed by FT-IR spectrometer. Sampling followed by filtration and lyophilization.

The first washing step was carried out using Triton X-100 (5g*L⁻¹). Followed by sodium carbonate solution (2g*L⁻¹). The last washing step was performed with distilled water. After drying the samples were transferred into 2 mL tubes for alkaline hydrolysis with sodium hydroxide. Incubation took place at 95°C for 30 min at 60 rpm in a shaking water bath. (Brueckner et al. 2008). The samples were taken during different phases of preprocessing. Samples as well as blanks (with/without carrier) were measured as triplicates. Sample preparation was performed according to previous samples.

Table 3: Alternative substrates for hydrolysis

Processing step	Sample Code
Liquid solution obtained after chemical hydrolysis step	EE21A
EE21A samples filtrated	EE21B
Solid residual from hydrolysis	EE21C

3.7.RP- HPLC

- The samples were analyzed at 600 bar and eluted at a volumetric flow rate of 0.75 mL/min. Absorption was measured at 241 nm.
- Analysis of the chromatogram and integration of the peak area was performed with “Agilent ChemStation software”.
- For the concentration, a standard calibration with TA and BHET was performed (Appendix). All samples were analyzed in triplicates.

3.7.1. Calibration curve

Due to the poor solubility of BHET in aqueous environment, the 1 mM BHET stock solution was prepared with MeOH and further diluted with MeOH instead of buffer. After addition of 500 µL equivalent reaction buffer, the samples were treated the same way as the TA calibration samples. Each calibration point was prepared as triplicate.

Table 4: RP-HPLC gradient

Time [min]	H ₂ O [%]	MeOH [%]	Formic acid [%]
------------	----------------------	----------	-----------------

1	80	10	10
8	40	50	10
10	0	90	10
15	0	90	10

3.7.2. Sample preparation

- The sample was mixed in a 1:1 ratio with ice-cold MeOH (Herrero Acero et al. 2011), followed by acidification with 1.5-10 μ L (depending on buffer used to prepare the sample) 6 molar HCl to a pH of ~3.5.
- The samples of one triplicate were acidified with the same volume
- The samples were then centrifuged at 14 000 rpm at 0 °C for 15 min followed by filtering them with a 0.45 μ m PA filter into a HPLC vial.

4. Results and Discussion

4.1. SDS-PAGE

As described in the material and methods section, the immobilization performed in this work, involved the covalent cross-linking between the amino groups from HiC lysines and the epoxy groups from beads. This bond could be involving any -NH_2 present in the interested environment. For this reason, the SDS-PAGE was performed.

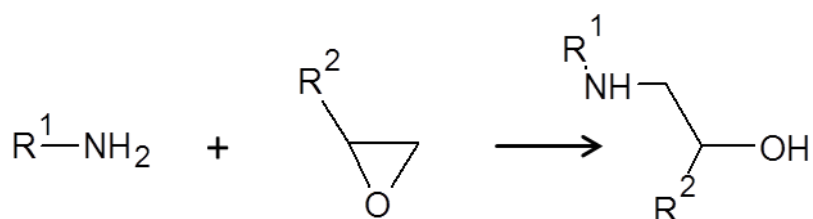


Figure 15: Simplified reaction of crosslinking between amino groups and HiC lysine residues. R^1 = Protein, R^2 = Carrier

In order to check eventual impurities in the enzyme solution, SDS-Page was performed. The sample in Lane 1 gives a signal at around 22 kDa which fits with the molecular weight as reported by Carvalho (Carvalho et al. 1998). As clearly shown in the figure, only one band was detected, meaning that no other protein is present and only HiC is linked to the carrier.

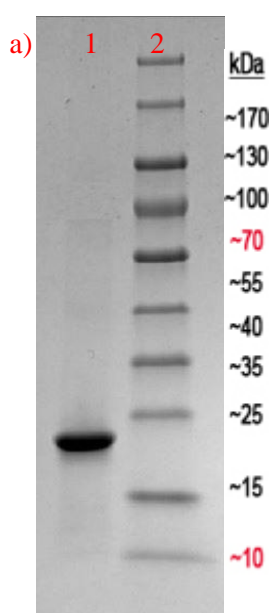


Figure 16: Gel scan of SDS-PAGE after Coomassie staining. a-1) HiC, Size standard, a-2) Protein Ladder PageRuler™

4.2. Activity and enzyme concentration

4.2.1. Immobilization

Figure 17 shows the advancing immobilization of the enzymes on the carrier material with a maximum of 86.6 % immobilized enzymes compared to the initial concentration before starting the reaction. After the first hour, already 71.3 % of the initial concentration was bound, which indicates a high affinity towards the carrier. Compared to immobilizations of HiC (A. Pellis et al. 2016) where an immobilization rate of >99% was achieved, this result is still sufficient when considering the age of the enzyme stock (A. Pellis et al. 2016).

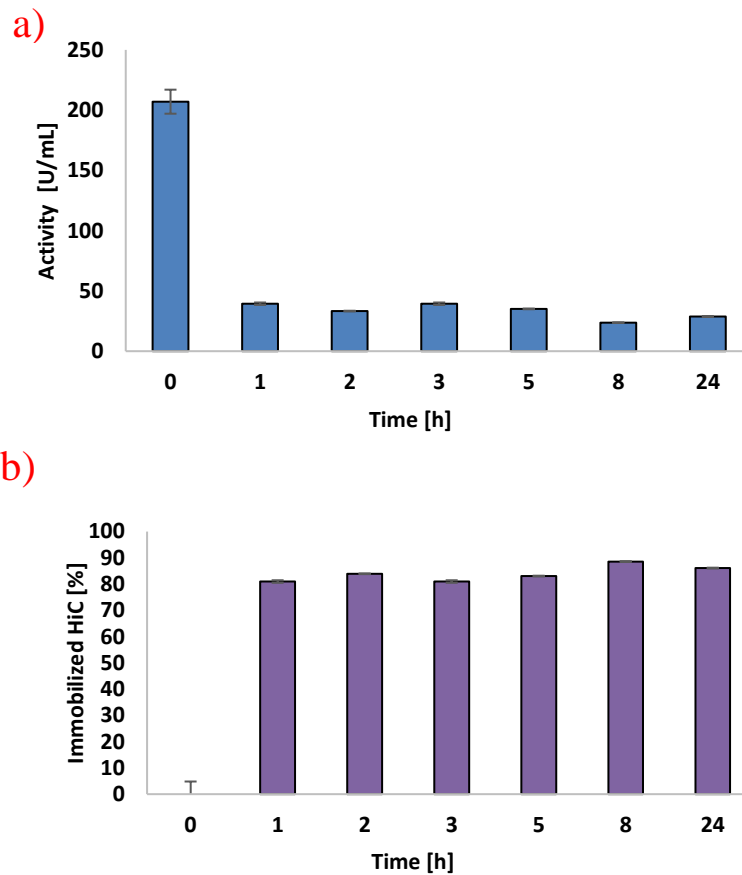


Figure 17: Monitoring of immobilization of HiC a) Enzyme concentration in the supernatant, b) Ration HiC immobilized (STD < 0.5%)

4.2.2. Activity of the immobilized enzyme

The rather low turnover of *p*-NPB substrate indicates a low activity. The mixture at 100rpm was not sufficient. Since iHiC was not reusable after this experiment and rather large amounts of *p*-NPB are necessary for this reason, all following activity essays were performed on the tecan reader on 96 well plates testing for leaching and activity of free enzyme.

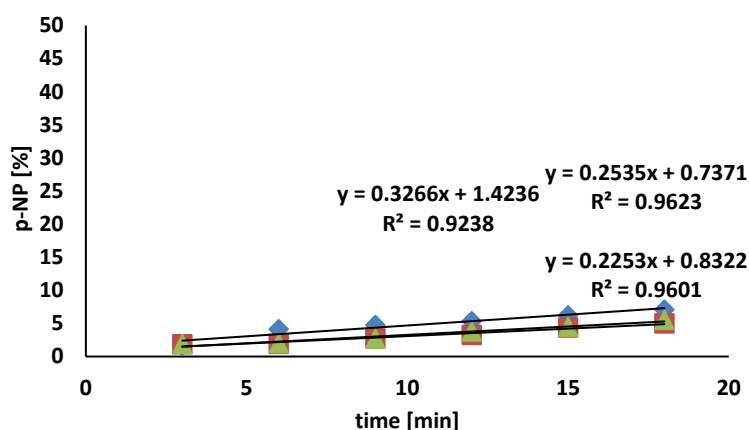


Figure 18: Released *p*-NP after incubation of *p*-NPB with iHiC.

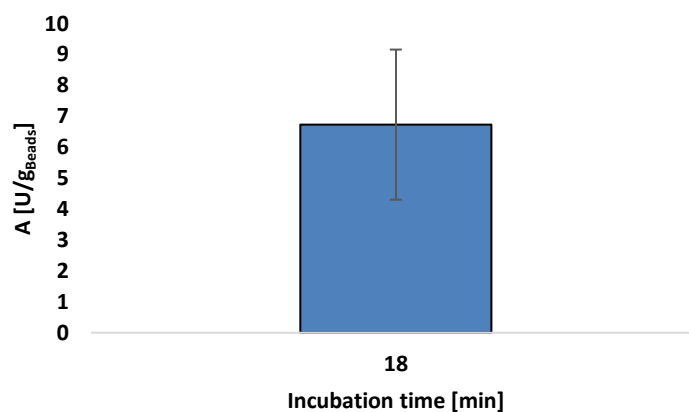


Figure 19: Activity of iHiC in U/gBeads

4.2.3. Long time leaching activity

In this section the activity was evaluated via *p*-NPB essay which was used to check whether the immobilized enzyme was leached or not. The activity of the leached enzyme in the supernatant was measured. Although the activity is rather small, even in the sample with the longest incubation time, enzyme activity could be measured. Although there is no direct correlation between leached enzyme

and released monomers, it was unexpected to find active enzyme because of leaching after more than 700h.

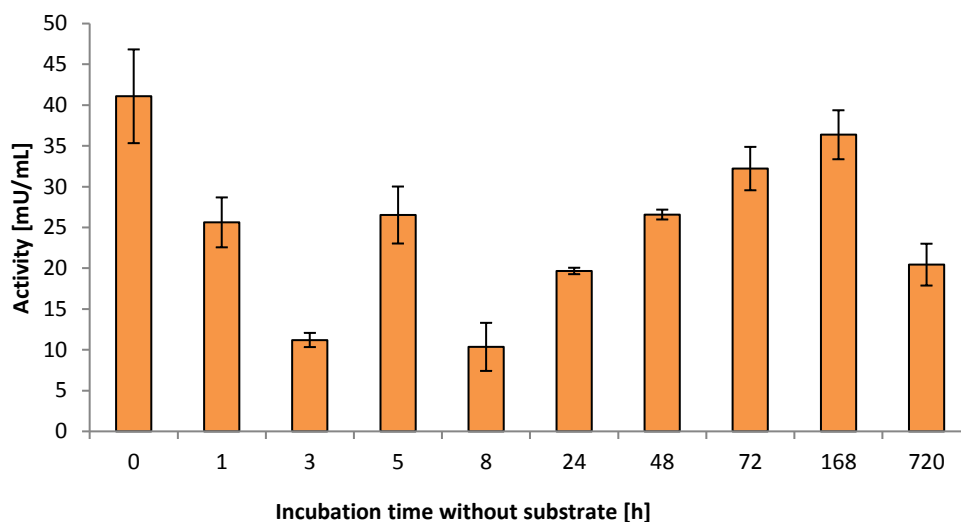


Figure 20: Activity of leached enzyme after long time incubation without substrate at 50°C 100rpm. Additional incubation with substrate of 72h und same conditions.

4.2.4. pH dependent leaching and activity (*p*-NPB activity assay)

In all experiments with different reaction buffers, the enzymatic activity of leached enzyme was almost exclusively measurable at pH 8.5. (Figure 21-25) This result could be reproduced in all experiments where the *p*-NPB activity assay was applied. As reported by Ronkvist *et al.* (Ronkvist et al. 2009) alkaline pH increases the activity of HiC especially at high temperatures. This could be verified as shown in Figure 23 and 27 where fHiC was incubated at 50°C and 70°C and the highest monomer release was measured at pH 8.5. When comparing the activity of iHiC and fHiC at 50°C the ratio between monomer release at pH 7 and 8.5 changed a lot, therefore it is unlikely that leaching took place at pH levels to the same extent. The activity of the leached enzyme at 70°C decreases after 72h as shown in Figure 23.

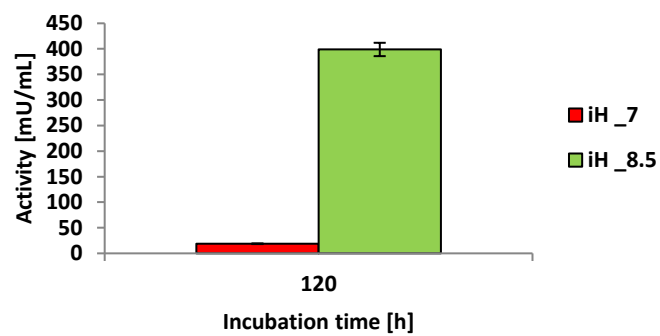


Figure 21: Enzyme activity of fHiC. Incubation at 50°C, 100 rpm.

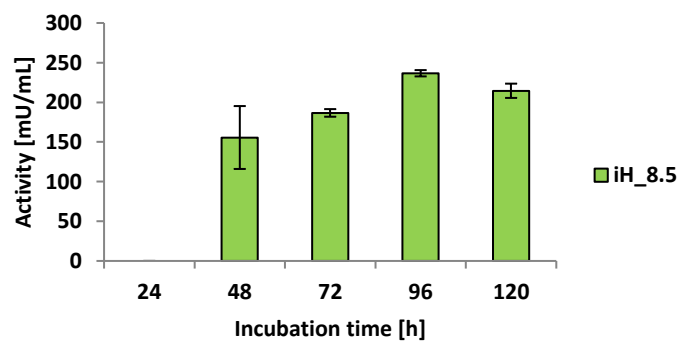


Figure 22: Activity of iHiC. Incubation at 50°C, 100 rpm.

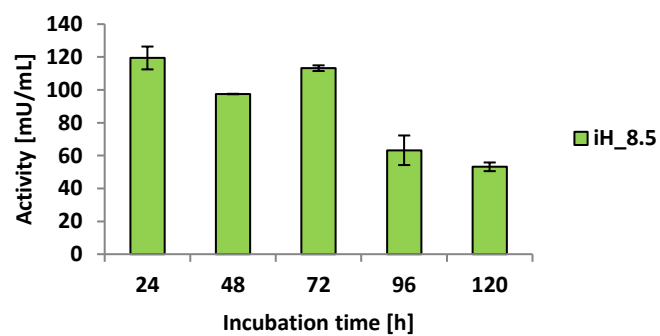


Figure 23: Activity of iHiC. Incubation at 70°C, 100 rpm.

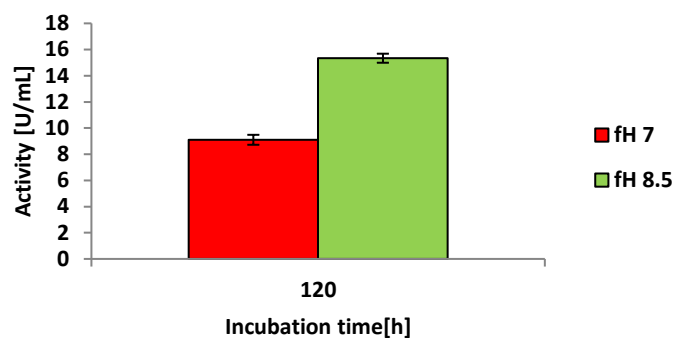


Figure 24: Activity of fHiC. Incubation at 50°C, 100 rpm.

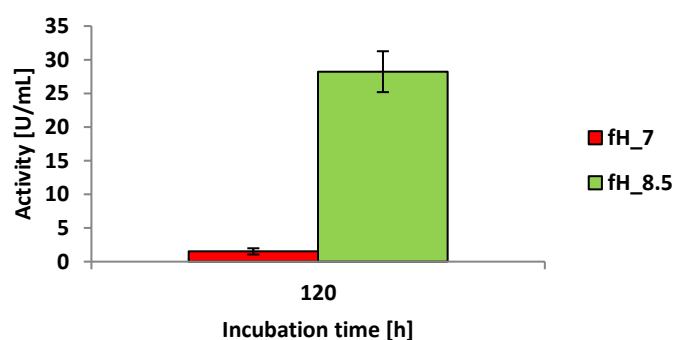


Figure 25: Activity of fHiC. Incubation at 70°C, 100 rpm.

4.2.5. pH dependent leaching and activity (*p*-NPA activity assay)

The last measures of enzyme activity were performed with *p*-NPA in order to check, if the length of the chain had any influence on the catalytic activity. The calculated activity was lower than for *p*-NPA. This time leaching was measured unlike previous experiments for pH 7, as well as pH 8.5, with a general maximum after 72 h of incubation.

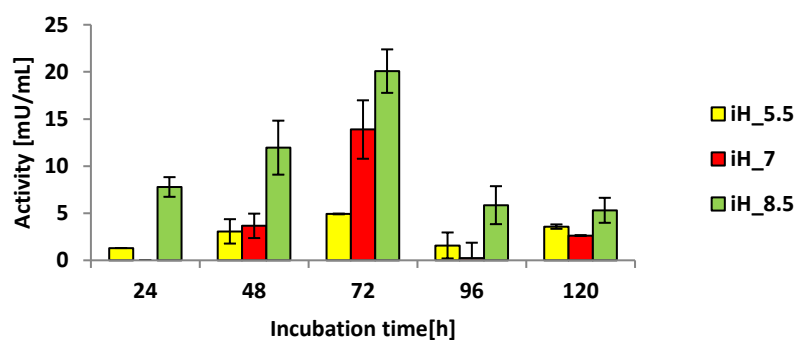


Figure 26: Activity of iHiC. Incubation at 50°C, 100 rpm. (*p*-NPA)

fHiC shows, as previously confirmed high activity at pH 8.5 although lower than in former experiments. A direct comparison to the repeated measurement of fHiC incubated at 0 rpm, 50°C (Figure 27 and Figure 25 revealed, that the activity at pH 7 decreased dramatically at °C 70 but gave the highest signal at 0 rpm and 50°C. The instability at pH 7 combined with high temperatures was observed again, as shown in Figure 28.

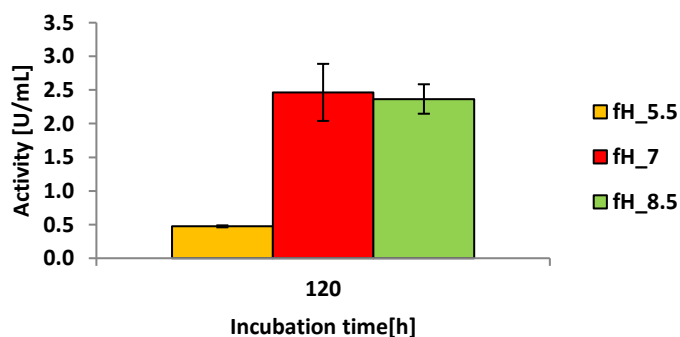


Figure 27: Activity of fHiC. Incubation at 50°C, 0 rpm (*p*-NPA).

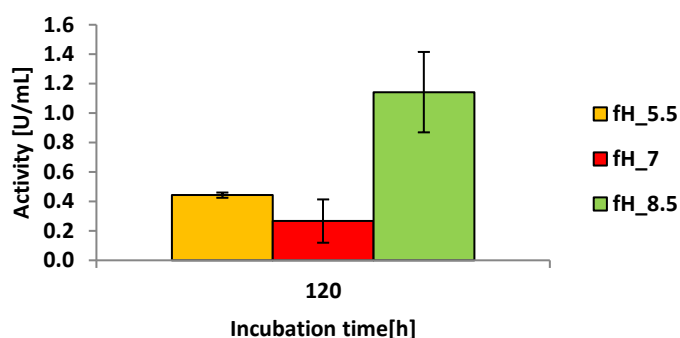


Figure 28: Activity of fHiC. Incubation at 50°C, 100 rpm. at 70°C, 100 rpm (*p*-NPA)

4.3.FT-IR analysis

Once defined the conditions of hydrolysis of PET model substrate using the immobilized enzyme, the aim of these experiments was to study the hydrolysis efficacy of immobilized *Humicola insulens* Cutinase when applied to preprocessed Resyntex samples from Umari with an inhomogeneous composition. Briefly, these Resyntex samples are mixture of oligomers obtained from the original polymers. As mentioned in the introduction, the aim was to apply the immobilized enzyme to hydrolyze only the PET oligomers without digesting oligo's from polyamide 6.6, which can be used as second value added chemicals. Those samples were obtained from the chemical hydrolysis of PET and Polyamide 6.6 under neutral condition (section 3.6.5). Before to start with the hydrolysis a spectroscopy study was performed FT-IR spectra (Figure 29), the solid samples EE21B and EE21C were compared to the spectra of pure PET and PA. PET shows the peak at $1,728\text{ cm}^{-1}$, indicative of ester bonds. This signal was considerably reduced during the chemical hydrolysis as shown in EE21B and EE21C. Correspondingly? the increase of the peak at 1690 cm^{-1} (typical of free $-\text{COOH}$ group) indicates the presence of oligomers of PET or TA in the mixture. On the other hand, the typical peaks of the amide I and amide II (respectively 1633 and 1538 cm^{-1}) confirm that also polyamide was partly degraded.

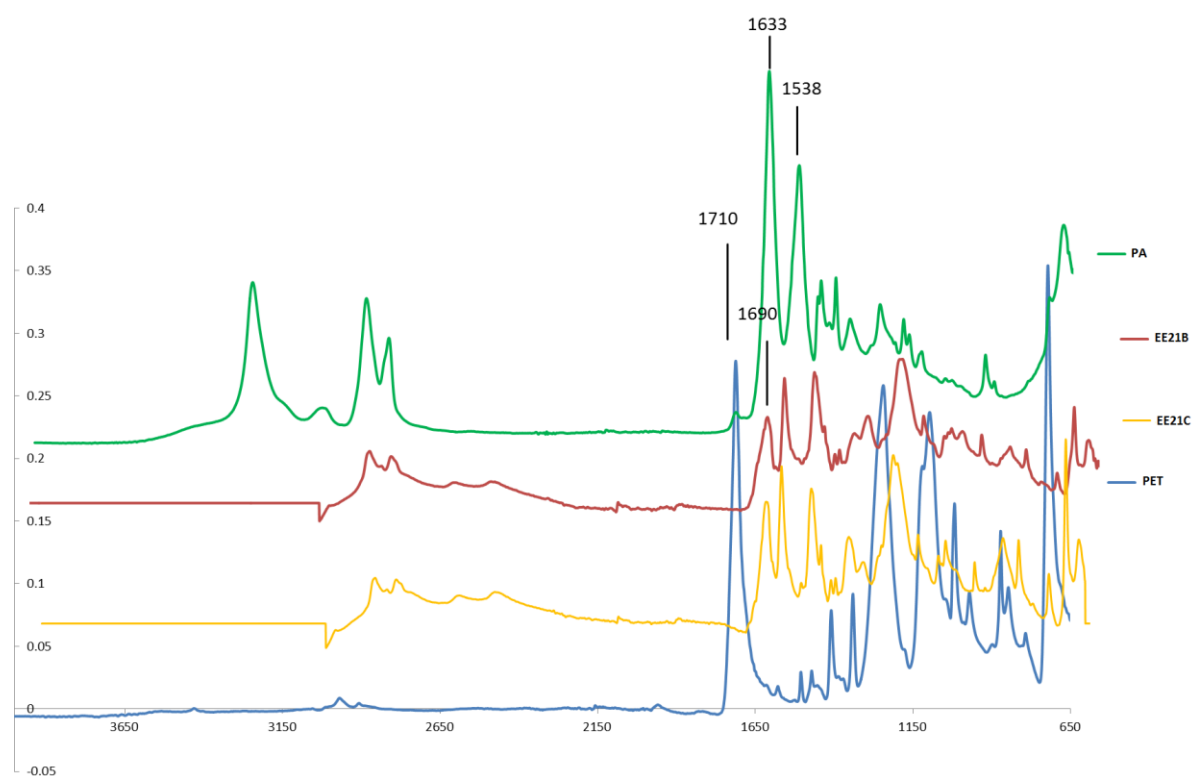


Figure 29: FT-IR spectra of Resyntex samples that were chemically preprocessed. EE21B) Filtrated and lyophilized solution obtained after chemical hydrolysis. EE21C) lyophilized solid residues after hydrolysis. Normalization area 2200-2000 cm^{-1}

The structural change that can also be observed, when PET is degraded to TA as shown in Figure 30. TA shows a peak at 1674 cm^{-1} indicating the presence of COOH groups, which was measured in the other sample as well. The characteristic peaks for polyamide are missing.

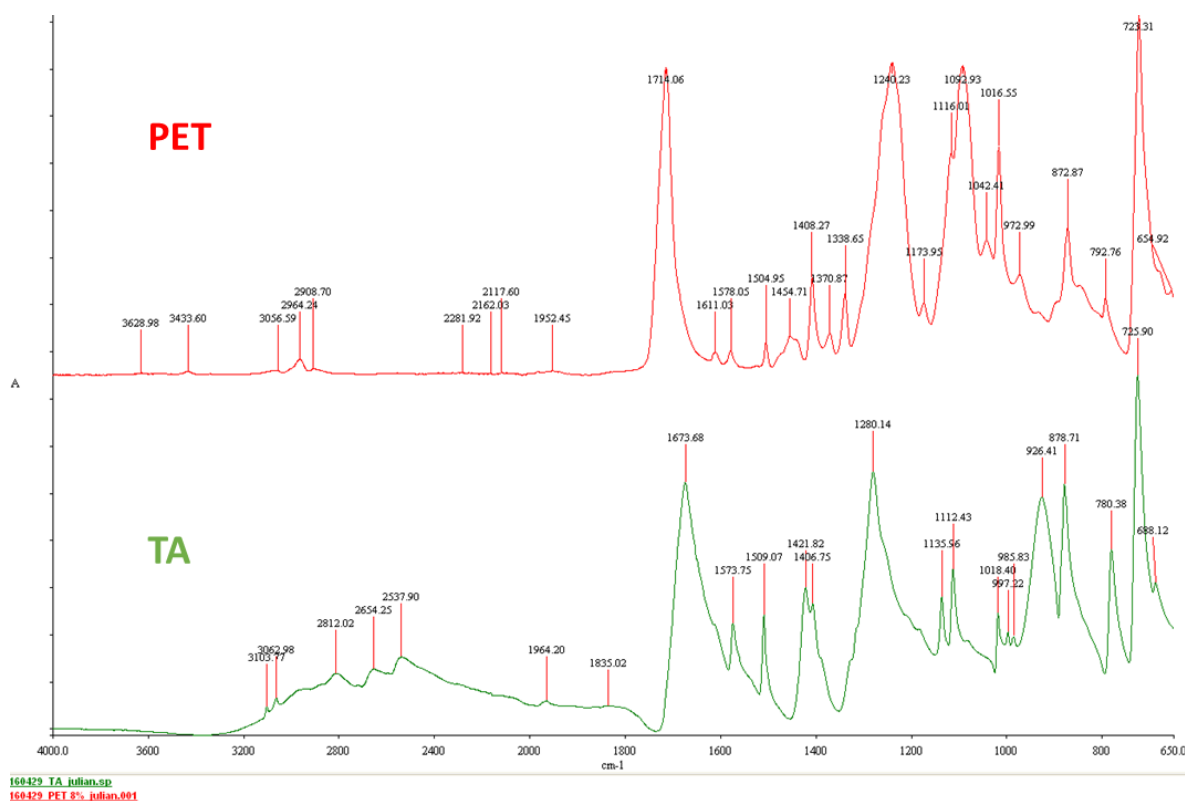


Figure 30: FT-IR spectra of PET powder and TA. Normalization area 2200-2000 cm^{-1}

4.4. RP-HPLC results

4.4.1. Washing stability

The effect of repeated rinsing with fresh buffer simulates the buffer exchange after incubation with substrate. This experiment helps to understand, how often the immobilized? enzyme can be reused. After washing of iHiC the concentration of TA after incubation for 24h was close to zero, nevertheless a very low concentration of MHET was still detectable. It seems that increased washing could have some influence on hydrolytic activity or that some of the enzyme was detached during the washing process.

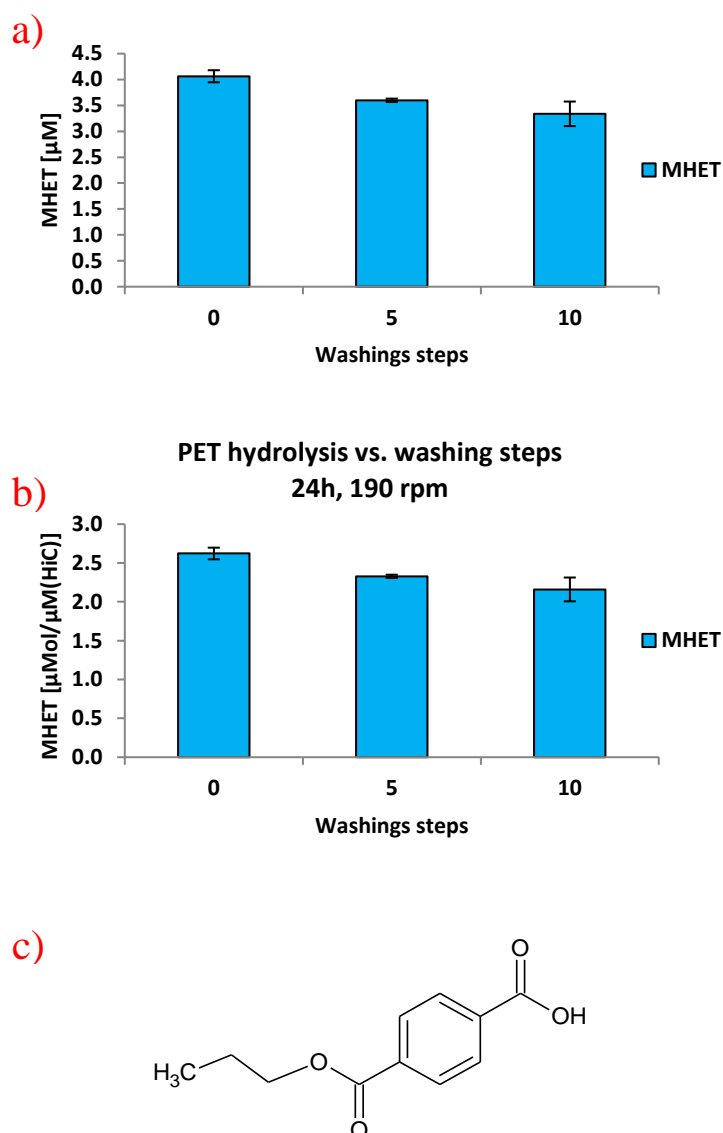


Figure 31: Effect of washing on hydrolytic activity of iHiC. a) Concentration MHET, b) specific product release MHET, c) chemical structure of MHET

4.4.2. Long time stability

The following results represent the most important outputs of the thermal stability experimental series. The only parameter which was varied thoroughly was incubation time. The objective was to find out the optimal time range for incubation with HiC to maximize the product yield.

Figure 32 shows the release of monomers over the time of incubation. To keep the activity of the enzyme regarding the target substrate comparable, only the last 3 days or 72 hours of incubation with substrate was performed. In every sample, the concentration of MHET is several times the one of TA, even within the last sample. The ratio is more or less constant (MHET/TA = 4.5-5.5). A possible explanation could be a product inhibition of MHET, which has been reported by

Wei (Wei et al. 2016). Since the general concentration is very low it can be assumed that insufficient interaction between enzyme and substrate was predominant.

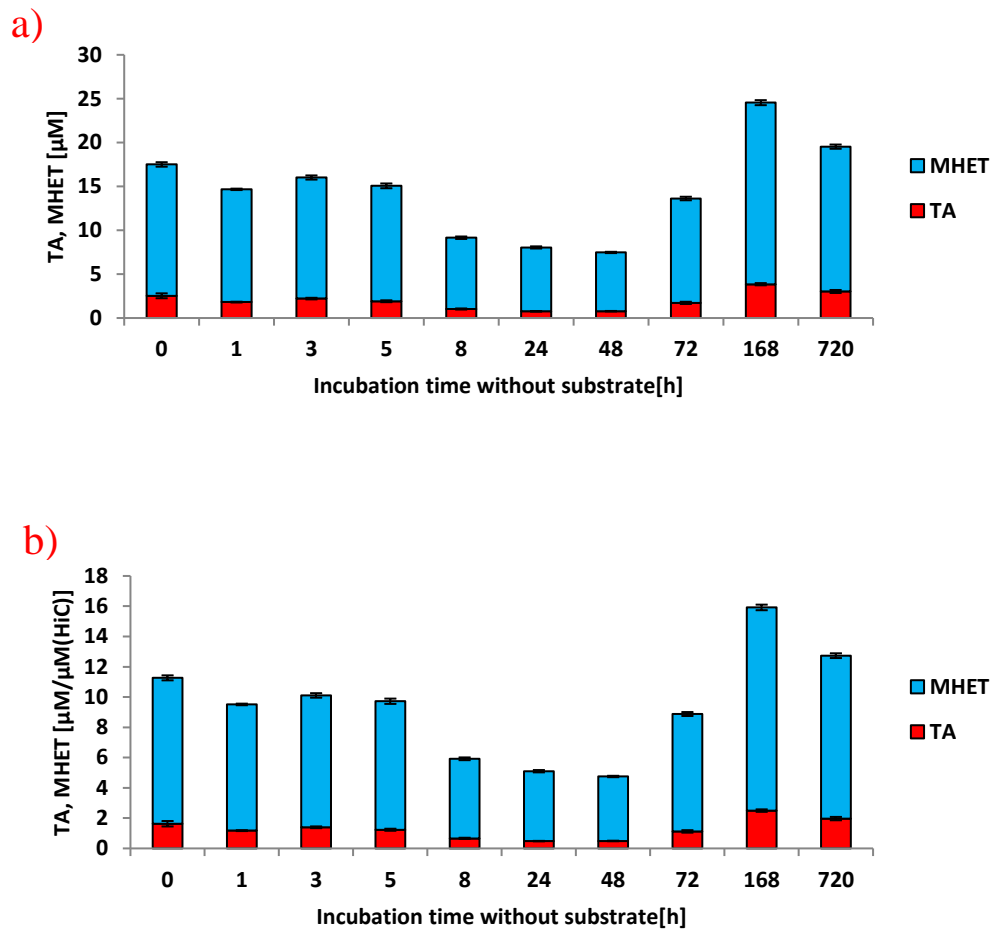


Figure 32: Long time incubation of PET powder with iHiC 100 rpm, 50°C. a) Concentration TA/MHET, b) specific product release TA/MHET, additional incubation with substrate of 72h und same conditions (STD < 0.5%)

4.4.3. pH stability

These experiments should verify whether acidic or alkaline conditions result in higher monomer release after incubation with immobilized and free enzyme. Temperature and rpm number where varied as well. After the testing, thermal stability and the influence of the buffer system in combination with pH shifts will give more information about the optimal incubation conditions for iHiC.

Figure 33 shows the release of monomers after hydrolysis of PET powder over a total time of 120h. The result shows only significant activity at pH 8.5 which confirms the data in section 4.2.4. No other reaction buffer shows a similar activity. Again, MHET seems to get accumulated stronger over time.

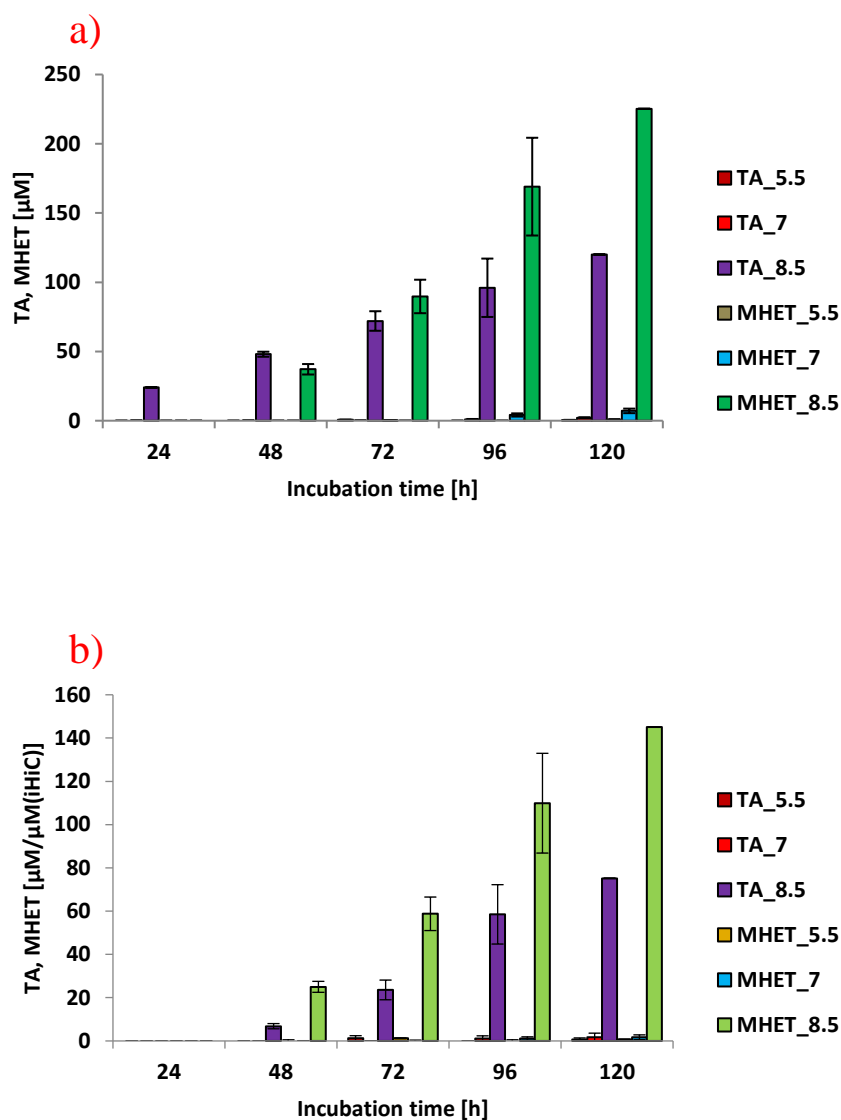


Figure 33: Incubation of PET with iHiC 100rpm, 50°C. a) Concentration TA/MHET, b) specific monomer release TA/MHET (no STD after 120h incubation time because of partial precipitation of monomers within sample triplicate)

At 0rpm similar results were achieved as demonstrated before but Figure 34 shows a higher ratio for TA meaning that pH 7 is apparently more suitable for iHiC.

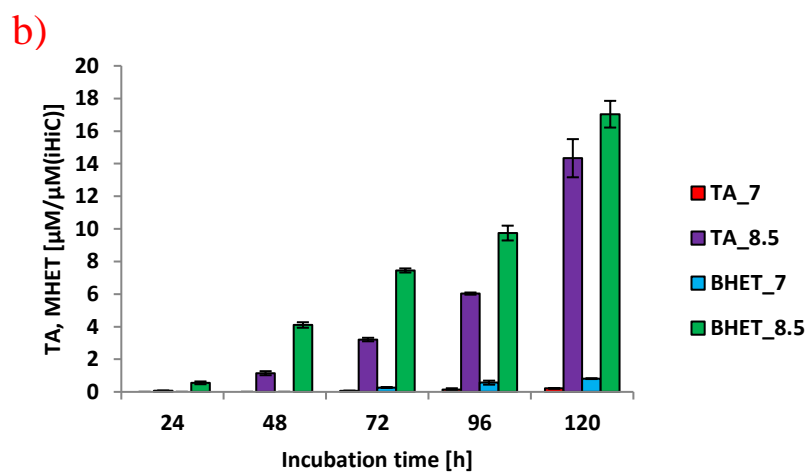
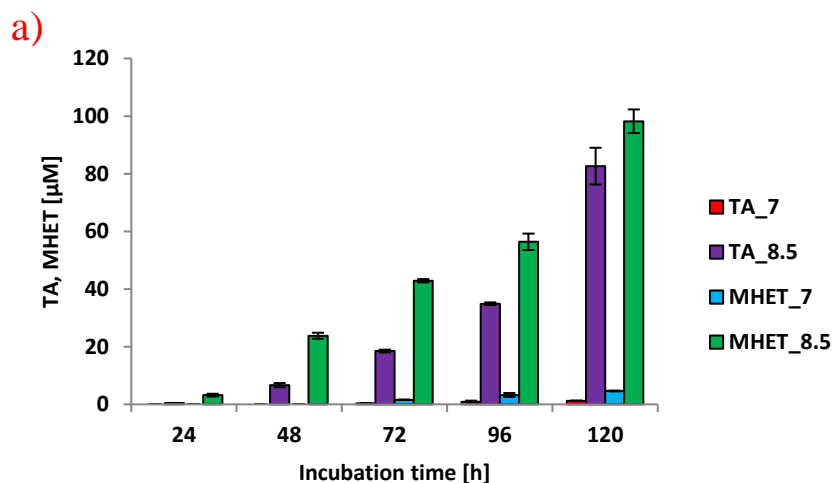


Figure 34: Incubation of PET with iHiC at 0rpm, 50°C. a) Concentration TA/MHET, b) specific monomer release TA/MHET

The concentration of released monomers after incubation with iHiC at 70°C dropped to 20% of the initial concentration in Figure 33. It seems that higher temperature does not improve the activity of the enzyme when immobilized.

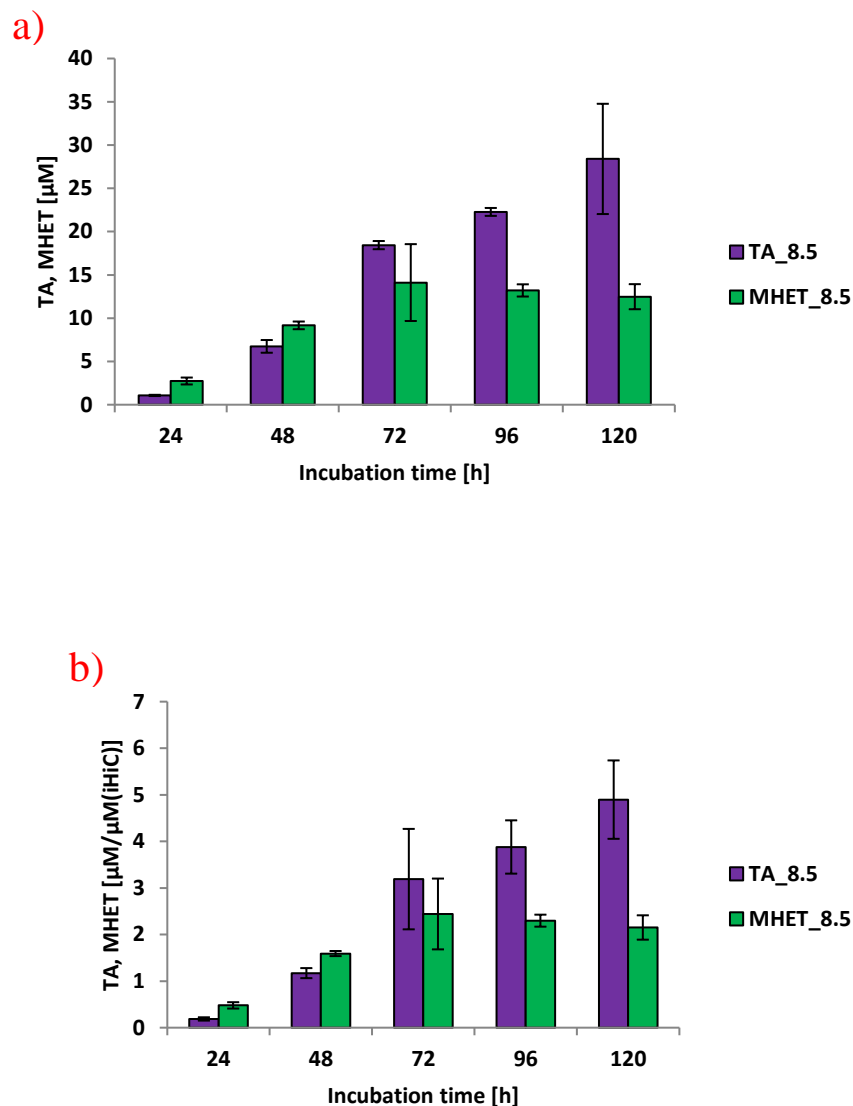


Figure 35: Incubation of PET powder with iHiC at 100rpm, 70°C. a) Concentration TA/MHET, b) specific monomer release TA/MHET

Without immobilization, the enzyme works far more efficiently as it has been shown in previous results. In Figure 36, the highest release occurred at the lowest pH, unlike the incubation with iHiC. The distribution of TA and MHET seems to be very different as well. Nevertheless, the relation between TA and MHET is comparable.

In the next experiment the significant influence of pH 8.5 could again be verified. As mentioned in section 3.6.4., this time 1.5 mL Eppendorf tubes for each time point were used instead of a 5 ml tube for all time points as described in section 3.6.3. The effective release of monomers in Figure 37 seems to be lower compared to the former experiment at 100 rpm which is most likely a consequence of variation of the experimental setting.

The incubation at 0 rpm, and therefore less mixing behavior and shear forces, led to lower monomer release in the samples with immobilized enzyme. It is likely, that additional movement enhances the leaching phenomenon at pH 8.5 and therefore limitations regarding diffusion of leached enzyme could have led to a lower reaction rate. As perceived in previous experiments, the monomer released at other pH levels is very low. The incubation with fHiC (see Figure 37) led to a different monomer distribution, although the overall amount of released hydrolysis products did not change extensively. It seems that without movement more TA was released than MHET which is preferable. This experiment has been repeated (see Appendix) with similar results.

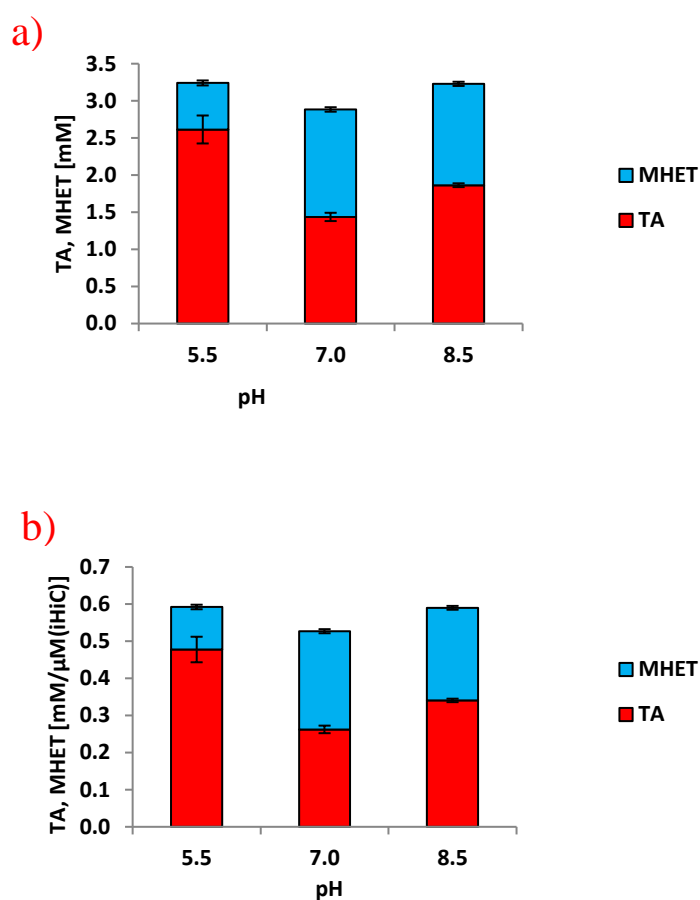


Figure 36: Incubation of PET powder with fHiC at 100rpm, 50°C. a) Concentration TA/MHET, b) specific monomer release TA/MHET

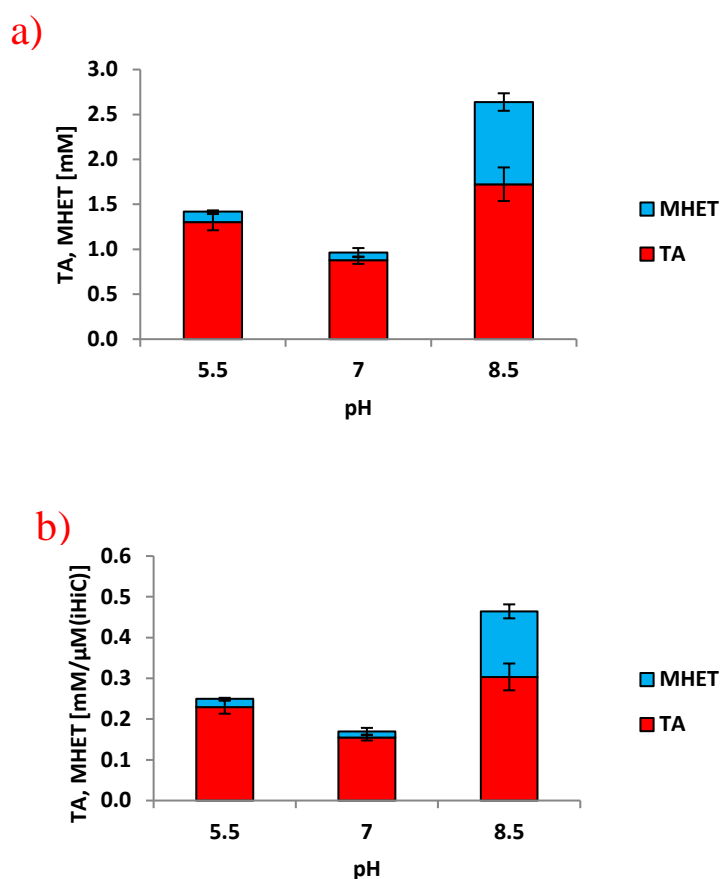


Figure 37: Incubation of PET powder with fHiC at at 0rpm, 50°C. a) Concentration of released Monomers, b) specific monomer release TA/MHET

The fHiC samples that were incubated at 70°C and pH 5.5, led to the highest concentration of released monomers that were measured. It can be considered that the near glass transition temperature (Saito and Nakajima 1959) significantly reduced the degree of order of the polymer as it has been reported and therefore increased the catalytic activity (Alves et al. 2002) as it has been demonstrated before (Ribitsch et al. 2012; Ronkvist et al. 2009) The biggest difference is the pH at which the peak of monomer release should be significantly higher. Regarding Literature pH 8.5 and 70-80°C are preferable (Carvalho et al. 1998; Petersen et al. 2001; Zimmermann and Billig 2010) but the group of Baker (Baker et al. 2012) reported the highest degradation rate of PCL at pH 5.0 and 40°C. So there is a chance that it also works for PET at 70°C.

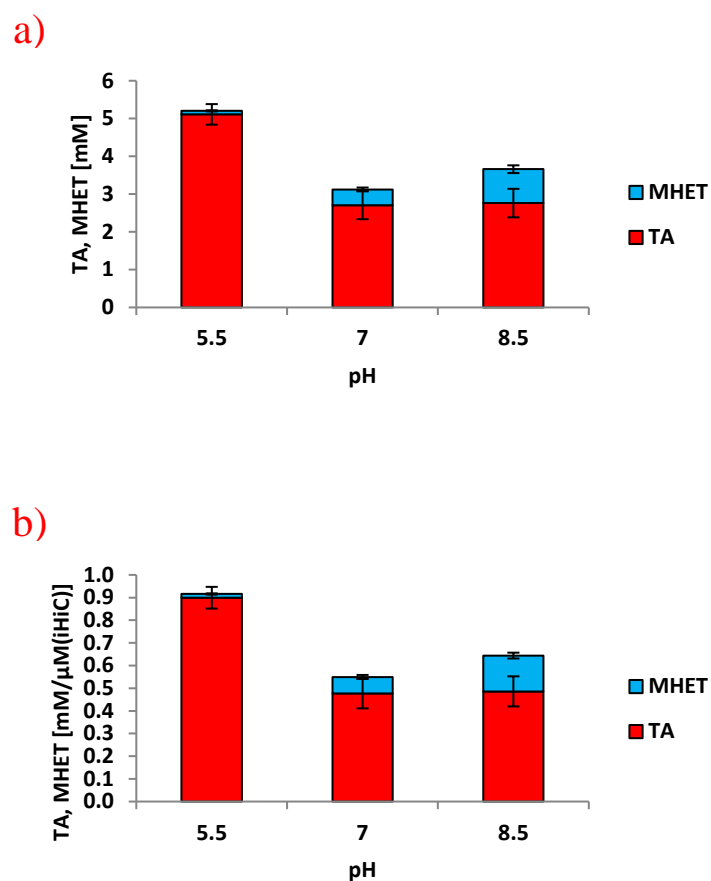


Figure 38: Incubation of PET powder with fHiC at 100rpm, 70°C. a) Concentration of released TA/MHET, b) specific monomer release TA/MHET

4.4.4. Variation of substrate ratios

A higher amount of substrate resulted in a slightly increased monomer release, but since the overall product concentration is very low the effect can be neglected. Nevertheless, it is plausible, that an optimized enzyme/substrate ratio will be beneficial for the process. In this experiment, only MHET was detectable

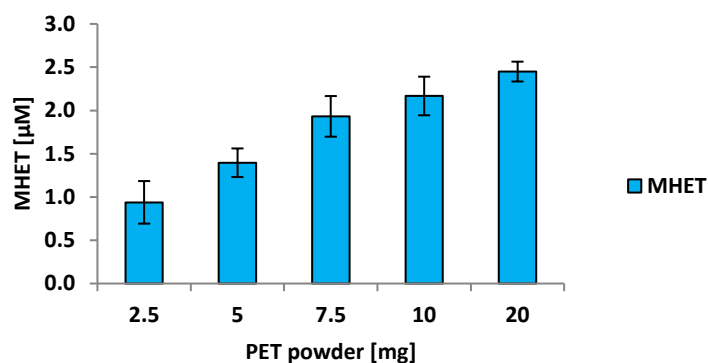


Figure 39: 2.5-20 mg of PET powder mixed with 10 mg of iHiC Substrate. Incubation with Tris/HCl 0.1M, pH 7 at 100rpm, 50°C

4.4.5. Hydrolysis of 3-PET

The incubation with the second model substrate, Bis(benzoyloxyethyl) with iHiC led to a much higher concentration of released monomers when compared to PET (Figure 41) again the highest concentration can be found at pH 8.5 but also notable monomer release at other pH levels. fHiC performed 5-10 times better and for the first time with a similar Monomer distribution as iHiC. This is promising since 3PET is water insoluble.

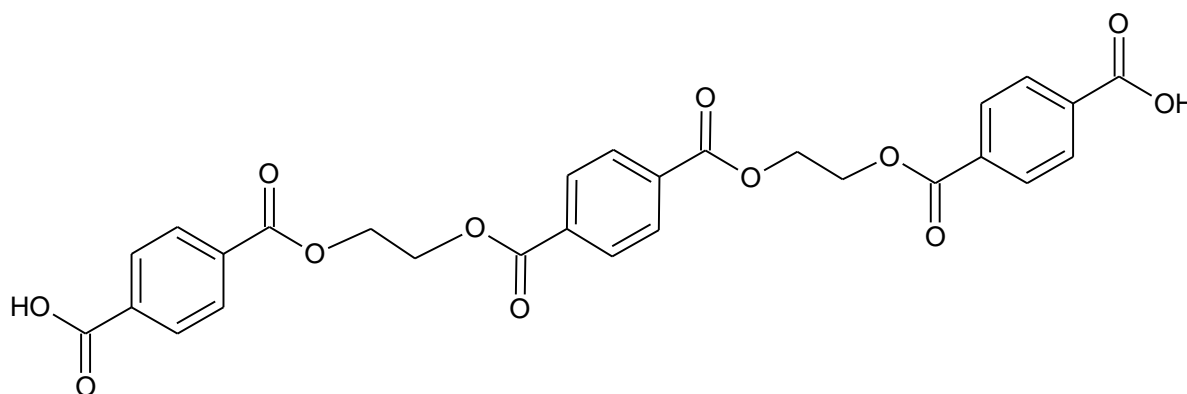


Figure 40: Chemical Structure of 3-PET

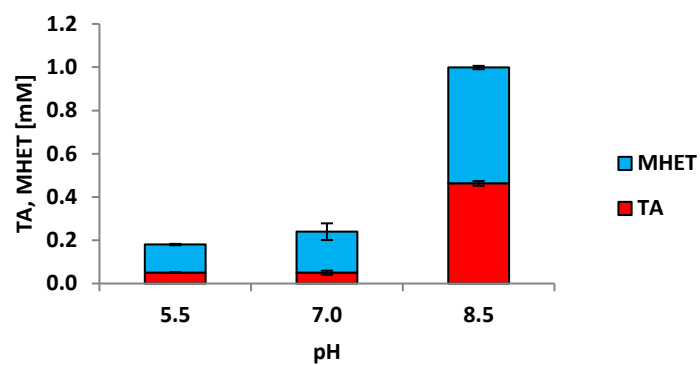


Figure 41: Incubation of 3-PET with iHiC at 100rpm, 50°C (no STD at pH 5.5 because of partial precipitation of monomers within sample triplicate)

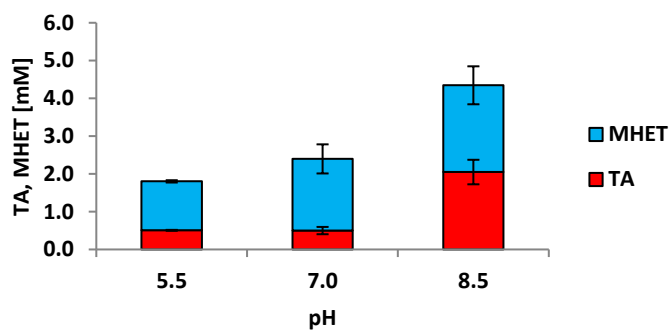


Figure 42: Incubation of 3-PET with fHiC at 100rpm, 50°C

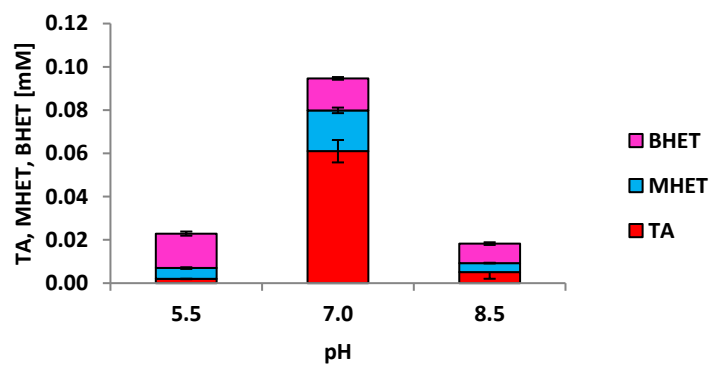


Figure 43: Blank of 3-PET. Incubation at 100rpm, 50°C

4.4.6. Hydrolysis of BHET

When incubated with a soluble substrate, iHiC (Figure 45) is able to completely degrade BHET into MHET and TA, though the fraction of TA is smaller. Although the total monomer release seems to be in the same range, incubation with fHiC (Figure 46) leads to full hydrolysis to TA. BHET seems to get instable when incubated at pH 8.5 as it can be seen in Figure 47 . Even without enzyme an almost complete conversion towards TA took place. This is an important criterion when considering enzyme activity at different pH levels. The highest stability for BHET was shown at pH 5.5 which also gave a good conversion rate for fHiC.

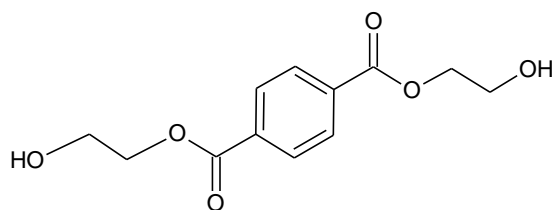


Figure 44: Chemical structure of BHET

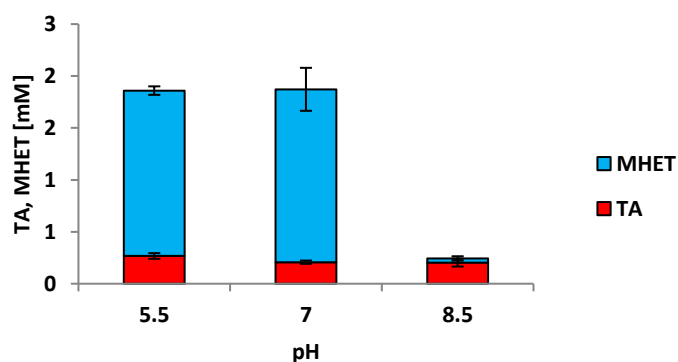


Figure 45: Incubation of BHET with iHiC at 100rpm, 50°C

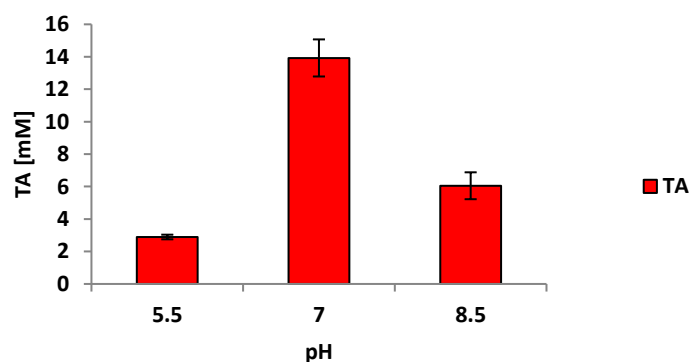


Figure 46 Incubation of BHET with fHiC (100rpm, 50°C)

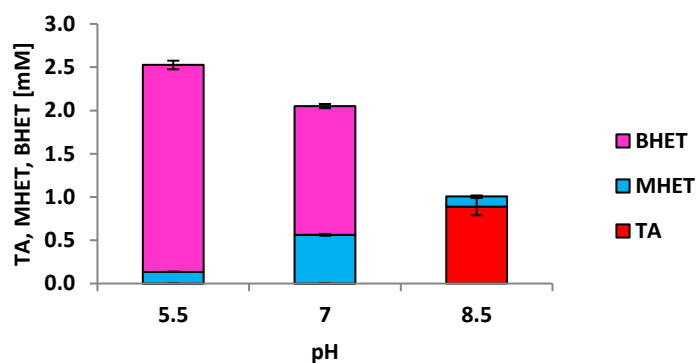


Figure 47: Blank-of BHET (100rpm, 50°C)

4.4.7. Hydrolysis of Resyntex samples

The incubation conditions tested in previous experiments with different model substrates were now applied for the incubation with chemically preprocessed PET fiber. After filtration (sample EE21B) MHET seems to be more stable since the Blank at pH 8.5 shows higher values than for the unfiltrated samples (EE21A) as shown in Figure 48 and Figure 49. Incubation with immobilized cutinase (Figure 50 and Figure 51) led to decrease of TA and MHET concentration, except for pH 7 in combination with sample EE21B which led to very good results. The inconsistent results can be a consequence of precipitation triggered by the inhomogenous composition of the sample material. At pH 8.5 the concentration of MHET was the same for blanks as for incubation with enzyme and significantly lower than at pH 5.5 and 7 which is most likely a result of the instability of MHET and BHET at alkaline conditions as demonstrated in section 4.4.5

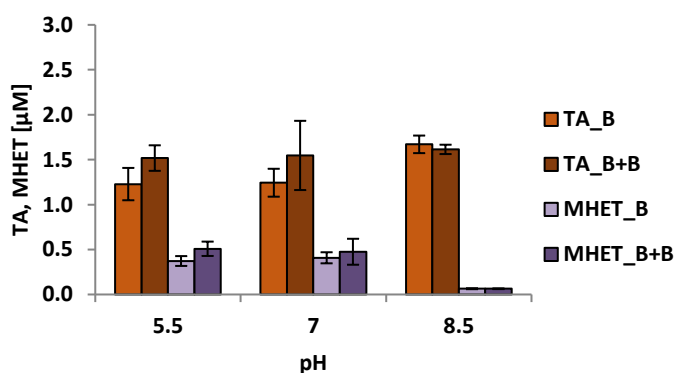


Figure 48: Blanks for incubation of chemically preprocessed PET fiber without filtration (EE21A). TA_B: Blank for TA (substrate + buffer). MHET_B: Blank for MHET. TA_B+B: Blank for TA + EC/EP beads, MHET_B+B: Blank für MHET + EC/EP beads

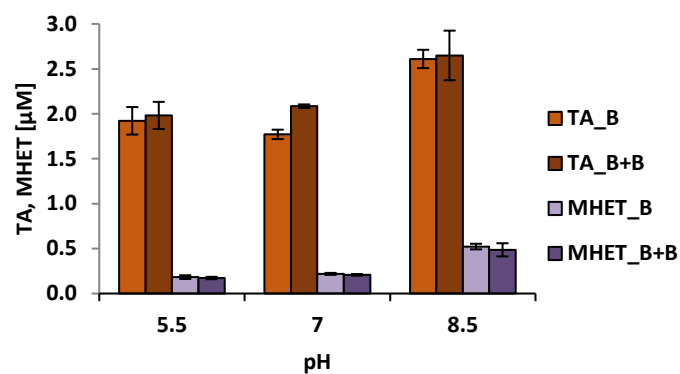


Figure 49: Blanks for incubation of chemically preprocessed PET fibre with filtration (EE21B). TA_B: Blank for TA (substrate + buffer). MHET_B: Blank for MHET. TA_B+B: Blank for TA + EC/EP beads, MHET_B+B: Blank für MHET + EC/EP beads

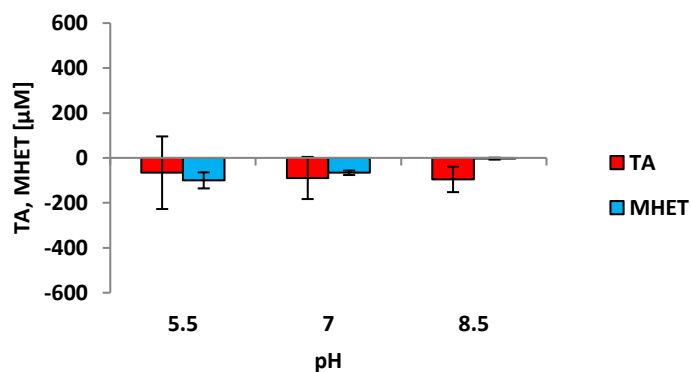


Figure 50: Incubation of lyophilized solution derived from chemically hydrolyzed PET fiber before filtration (EE21A) with iHiC at 100rpm, 50°C

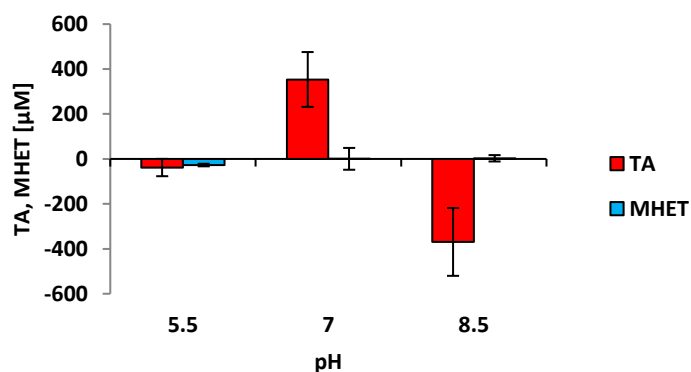


Figure 51: Incubation of lyophilized solution derived from chemically hydrolyzed PET fiber after filtration (EE21B) with iHiC at 100rpm, 50°C

Incubation with free cutinase lead to slightly better results. No MHET was detected which means that this fraction was fully converted to TA by the enzyme. Unlike for the immobilized enzyme. Filtration did not improve the result this time. Only at pH 5.5 an increase of hydrolysis product was measured. The concentration of TA at pH 8.5 went down instead of up. In addition, a high standard deviation was obtained.

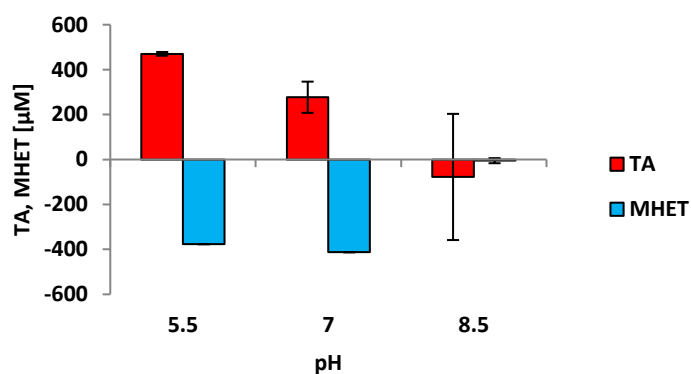


Figure 52: Incubation of lyophilized solution derived from chemically hydrolyzed PET fiber before filtration (EE21A) with fHiC at 100rpm, 50°C (no STD at pH 5.5 and 7 because of partial precipitation of monomers within sample triplicate)

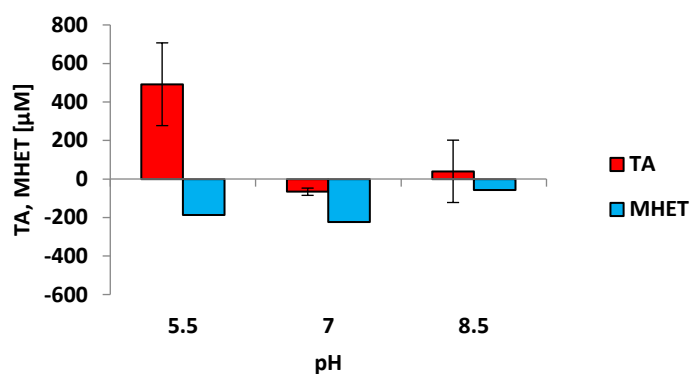


Figure 53: Incubation of lyophilized solution derived from chemically hydrolyzed PET fiber after filtration (EE21B) with fHiC at 100rpm, 50°C (no STD after 120h incubation time because of partial precipitation of monomers within triplicate)

5. Conclusions and outlook

The objective of this thesis was to identify optimal reaction parameters for incubation of the model substrates PET, 3-PET and BHET with immobilized cutinase. This was followed by examining the potential of iHiC to hydrolyze chemically pre-processed PET fiber and comparing the results to previous gained data.

Although the activity of immobilized *Humicola insolens* cutinase was lower than for the free enzyme, no activity loss was measured during long time incubation. The inhibitory effect of MHET as reported by Barth *et al.* (Barth et al. 2015) was observed but could be overcome with a dual enzyme concept similar to the one developed by the same group, where TfCut2 from *Thermobifida fusca* hydrolyses the PET to MHET and metagenome-derived TfCut2, LC-cutinase (Wei et al. 2012) further degrades the intermediate product to TA. The unexpected effect of enzyme activity in the reaction buffer after incubation with iHiC at pH 8.5 suggests that pH specific leaching occurred: On the one hand, activity was measured after incubation of fHiC at pH 7 under the same conditions as for iHiC, where almost no activity as measured, on the other hand no hydrolysis products were found after incubation of iHiC at 70°C and pH 5.5 but led to the highest release of TA when fHiC was used. Regarding literature (Mateo et al. 2000) alkaline pH should not affect the binding stability since the multipoint attachment of the enzyme with epoxy linkage is unlikely to break that easily. A possible explanation can be the detachment of adsorbed enzyme that was not covalently bound as a consequence of pH driven conformational change. This means that the washing at pH 7 might not fully remove the unbound enzyme after immobilization. The absence of shaking led to a lower activity for iHiC most likely as a result of a concentration gradient of the leached enzyme. The optimum incubation time for HiC seem to be 72h since activity of leached enzyme drops after when incubated for longer time periods (section 4.2.4 and 4.2.5).

Free *Humicola insolens* cutinase on the other side seemed to have comparable activity at all tested pH levels with the highest release of TA at pH 5.5. at 70°C, this differs from pH optima for PET degradation as discussed in section 4.4.3. Behavior of HiC in acidic condition at high temperature needs to be examined more closely. Influence of shaking was neglectable with no significant change in monomer distribution.

The efficiency of iHiC increased dramatically when applied to the insoluble model substrate 3-PET blank showed minimal and therefore neglectable instability of the substrate at neutral pH. The concentration increased 10-fold when fHiC was used for incubation, although monomer distribution and pH behavior were similar to the immobilized enzyme. This time a clear preference for pH 8.5 was observed. The soluble hydrolysis product BHET was an excellent substrate for iHiC as expected, although accumulation of MHET was inevitable. Incubation of fHiC led to full degradation (Figure 46).

The destabilizing effect of pH 8.5 on BHET as demonstrated in Figure 47 needs to be taken into consideration when evaluating the performance of the enzyme at this pH.

Regarding the chemically preprocessed samples from the university of Maribor, precipitation and adsorption enhancing effects due to impurities could have had a negative effect on the solubility of the released monomers after incubation with immobilized as well as free enzyme. When comparing the reaction samples to the blanks without enzyme, the concentration went down instead of up for iHiC. A relatively high release of TA monomers after incubation with iHiC was measured with EE21B at pH 7 which was even comparable with the result for fHiC. This is remarkable since no other condition lead to TA monomer concentration this high and a good indicator to stay with pH 7 and 50°C when using immobilized HiC for chemo enzymatic hydrolysis. Filtration of the samples seems to be crucial to reduce possible precipitation as demonstrated.

The high standard variation indicates that the individual composition of the sample greatly affects precipitation. Since free enzyme might precipitate in presence of inhomogeneous sample composition, immobilized *Humicola insolens* cutinase is preferable for complex samples.

6. Appendix

1) Laboratory facilities

pH meter	Microprocessor
	WTW (Germany)
Balance	Scaltec (Germany)
	Aventurer TM (Canada)
Pipettes 100/200/1000 µL	Gilson (France)
Pipettes 10µL	
Flask 100 mL	Duran Group (Germany)
	?
Flask 500 mL	Duran Group (Germany)
Beaker 50 mL	Duran Group (Germany)
Beaker 100 mL	Duran Group (Germany)
Beaker 250 mL	Duran Group (Germany)
Beaker 500 mL	Duran Group (Germany)
Ultracentrifuge Sorval lynx 4000 label 2	Thermo fisher scientific
Plate Reader Tecan Infinite Pro	Tekan (Switzerland)
Incubator INFORS HT Multitron	INORS AG (Switzerland)
Digital Sonifier	Branson Ultrasonic Corporation (USA)
Chemidoc	Biorad (USA)
HPLC “Ultimate 3000 Autosampler Dionex	Thermo Scientific (USA)
FT-IR	Perkin Helmer

2) Methods

2.1) SDS-PAGE

Sodiumdodecylsulfate Polyacrylamide-Gel electrophoresis or SDS-PAGE is a technique to separate Proteins regarding their size as first practiced by Laemmli (Laemmli 1970). This technique is widely used in different field such as Biology, biochemistry, forensics or genetics. It's simple application and analysis qualifies it for a wide range of applications. The separation process is based on forcing the polypeptide chain of a protein through a polyacrylamide gel slows down larger proteins more

strongly than shorter proteins. The sample can be applied in their native state to preserve their higher order structure or in denaturated stage. If a reduced sample is preferable, a reducing agent like β – Mercaptoethanol is added to reduce the disulfide bridges which lead to a linearization of the polypeptide chain. The SDS binds to the it and leads to an all over consistent charge per unit mass value so that the

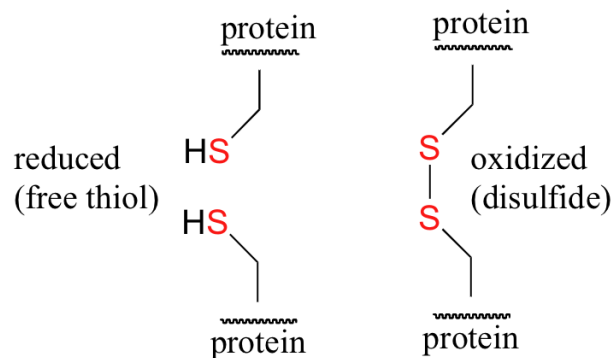


Figure 54: Reduction of disulfide bonds

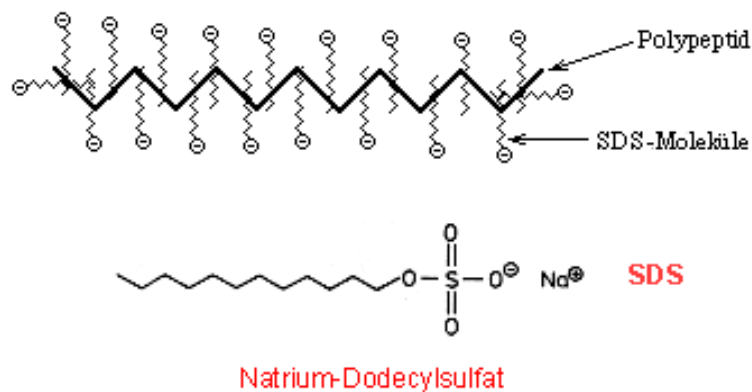


Figure 55: Effect of SDS on polypeptide chains

migration velocity is only size dependent. One big disadvantage is the fact that the biological activity is destroyed when applying this technique. Further analysis can be done via western blotting or staining

Composition of Laemmli buffer (4x) (Biorad):

Tris_HCl, pH 6.8	277.8 mM
Glycerol	44.4% (v/v)
LDS (lithium dodecyl sulfate	4.4%
Bromphenol blue	0.02%

2.2) FT-IR spectroscopy

Infrared spectroscopy as a technique where the molecular structure of a sample is analyzed via adsorption of infrared radiation. Different chemical bonds have characteristic spectra where resonance can be measured. The adsorption of energy occurs at frequencies that are corresponding to vibration of the molecular structure which is dependent on the chemical bond or group. The most usable IR region corresponds to the mid-IR spectrum (between 4,000 and 400 cm^{-1}) (Alvarez-Ordóñez and Prieto 2012). An active IR-molecule undergoes a change in dipole movement as a result of its induced movement. Each of these vibrational modes has a specific vibration pattern correlating to the mass of atoms and the strength of the chemical bond, which connects them. Larger masses tend to have a lower frequency whereas stronger bonds lead to a higher frequency.

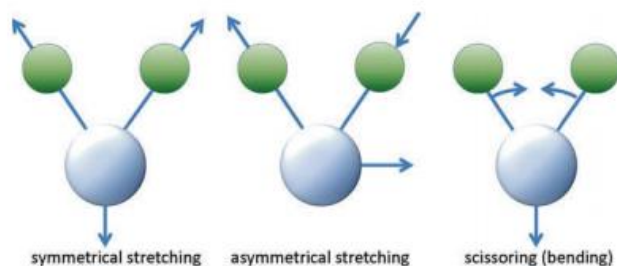


Figure 56: Types of movement induced by infrared radiation (Alvarez-Ordóñez & Prieto 2012)

The FT-IR spectrometers were invented in the 1960s but did not find frequent application during that time due to high costs. With advancing technology, the devices became cheaper and are now used in many different fields.

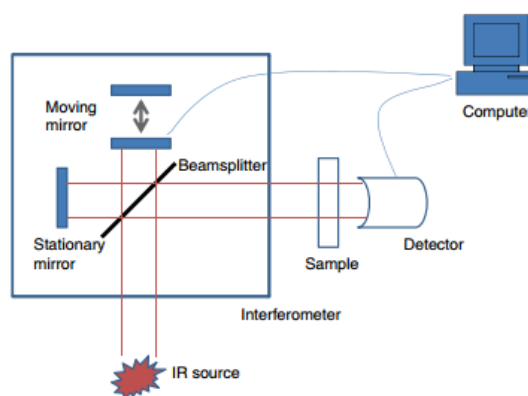


Figure 57: Basic components of an FT-IR spectrometer (Alvarez-Ordóñez and Prieto 2012)

The source of IR radiation can be a Nernst glower (based on rare earth oxides), Globar source (rod of silicon heated electrically), or a carbon dioxide laser. Although they emit continuous radiation, they have different energy profiles, which leads to different possibilities for application. The essential components of each FT-IR spectrometer are the light source, the detector, and a Michelson interferometer (consists of a moving mirror, a fixed mirror, and a beam splitter). The interferometer produces a characteristic interference signal when an IR beam passes through the sample. The measured signal results in an interferogram that is mathematically transformed from the time domain to the frequency domain.

2.3.) Calibration Bradford assay

Two calibration rows have been used:

Table 5: BSA calibration 1

Conc. standard [$\mu\text{g/mL}$]	V(Stock) [μL]	V(Buffer) [μL]
500	300	900
400	240	960
250	150	1050
200	120	1080
100	60	1140
50	30	1170
25	15	1185
12.5	7.5	1192.5

Table 6: BSA calibration 2

Conc. standard [$\mu\text{g/mL}$]	V(Enzyme) [μl]	V(Buffer) [μL]	Code
1000	500 (stock)	500	A
500	500 (A)	500	B
250	500 (B)	500	C
125	500 (C)	500	D
62.5	500 (D)	500	E
31.25	500 (E)	500	F
200	100 (stock)	900	G
100	500 (G)	500	H
50	500 (H)	500	I
25	500 (I)	500	J

A linear regression of the data points was performed to obtain an equation to correlate the absorption at 595 nm with the protein concentration. All calibration samples were measured in triplicates.

2.4) *para*-Nitrophenyl substrate) activity assay

The enzymatically catalyzed addition of a water molecule to the-NPB molecule leads to a cleavage into Nitrophenyl which absorbs at 405 nm and butyrate. This assay is used to determine the activity of esterases. A limitation of the technique is its poor performance at low pH. The substance is very light and temperature sensitive. The reaction with *p*-NPA as substrate follows the same principle.

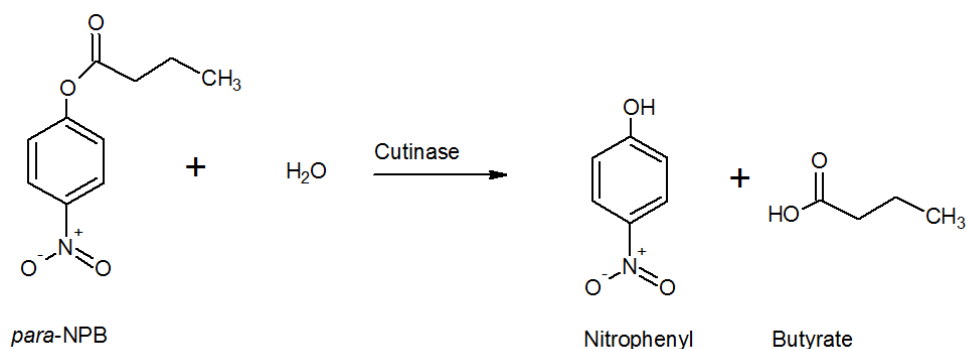


Figure 58: Hydrolysis of the substrate molecule

2.5) HPLC

High performance liquid chromatography or HPLC is a technique for separating molecules via hydrophobic interaction under high pressure (300-400 bar). The advantage of this extreme pressure is a relatively high purification rate within a short time. The solid phase of the column has a very fine structure this results in an increased surface and intensified interaction with the analyte. After the separation or purification a detector measures the concentration of the analyte in the eluate. (Letzel 2010)

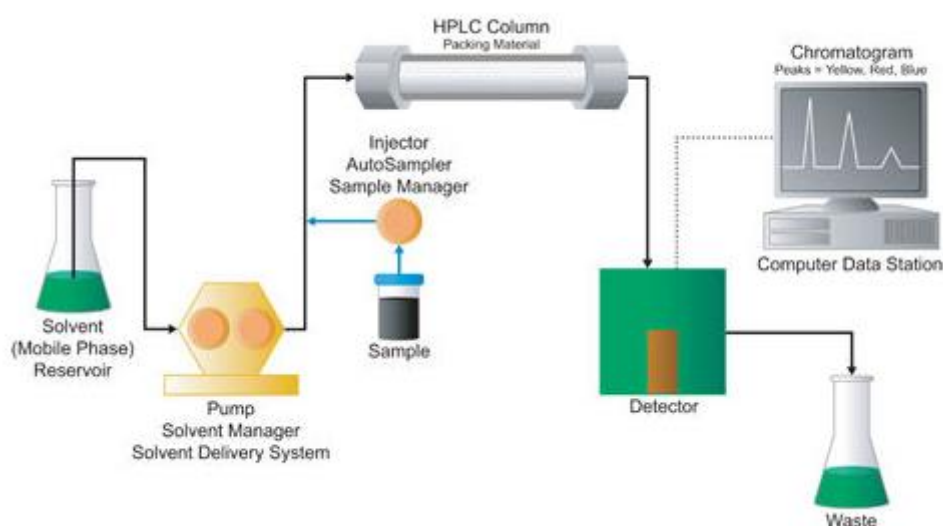


Figure 59: setup of a HPLC system (Waters 2017)

2.6) Calibration of HPLC

The concentration of TA and BHET was exclusively measured with reverse phase HPLC. Standard calibrations were measured with an increasing concentration beginning with the lowest. A calibration curve of terephthalic acid for each desired pH was obtained by creating 1mM stock solutions with TA dissolved in NaAc 0.1 M, pH 5.5; Tris/HCl, 0.1 M, pH 7 or Tris/HCl 0.1 M, pH 8.5. After addition of the buffer, the samples were mixed with ice cold MeOH, centrifuged at 14 000 rpm at 0 °C for 15 min followed by filtering them with a 0.45 μ m PA filter into a HPLC vial. Each calibration point was prepared as triplicate.

Table 7: Standard calibration TA

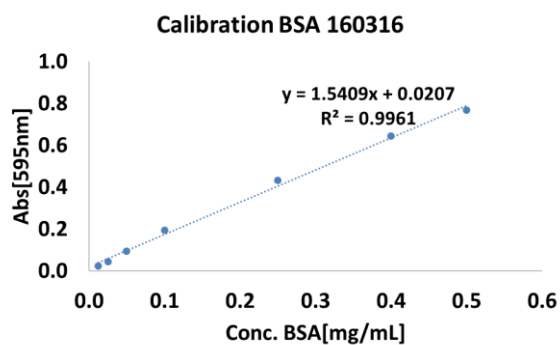
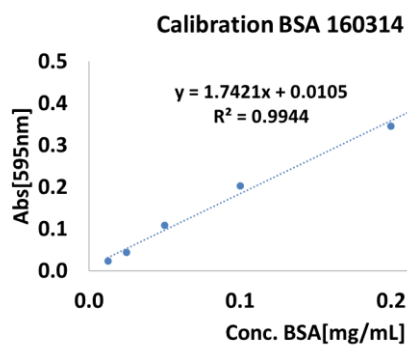
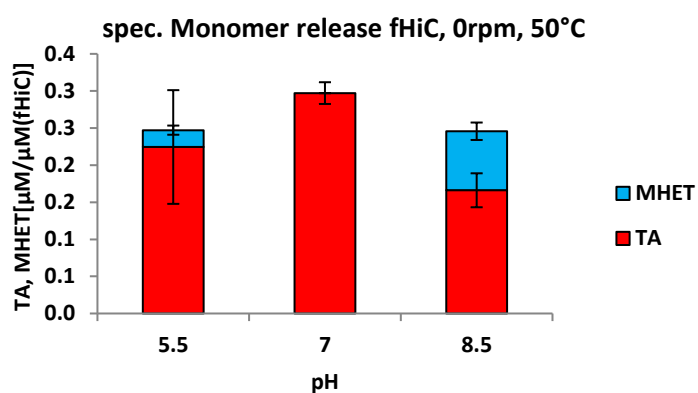
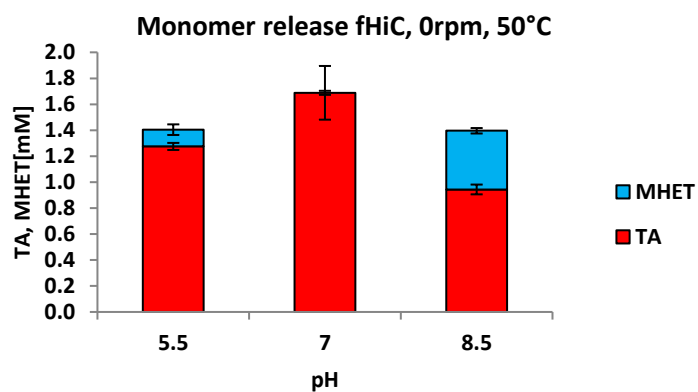
Conc.[μ M]	1 mM TA [μ L]	Buffer [μ L]	MeOH [μ L]
500	500	0	500
250	250	250	500
100	100	400	500

50	50	450	500
10	10	490	500
5	5	495	500
1	1	499	500

Table 8: Standard calibration BHET

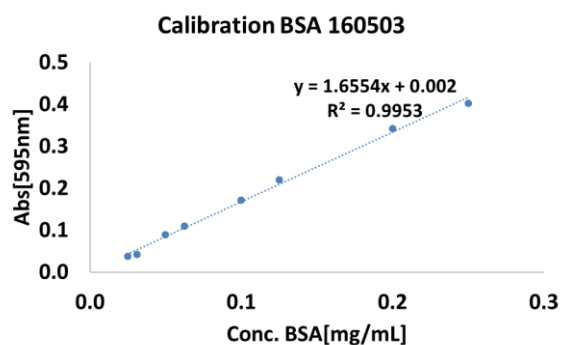
Conc.[μM]	1 mM BHET [μL]	MeOH [μL]	Buffer [μL]
500	500	0	500
250	250	250	500
100	100	400	500
50	50	450	500
10	10	490	500
5	5	495	500
1	1	499	500

2) Results

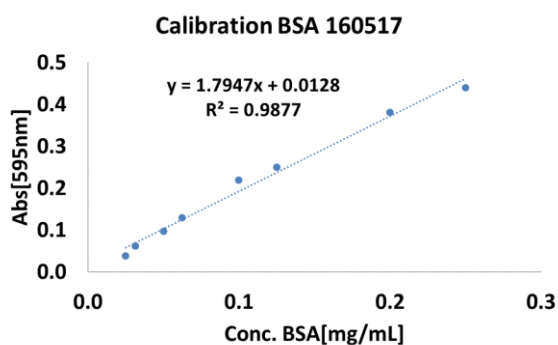


L.O.D[Abs]	L.O.Q[Abs]	L.O.D[mg/mL]	L.O.Q[mg/mL]
0.023	0.054	0.008	0.839

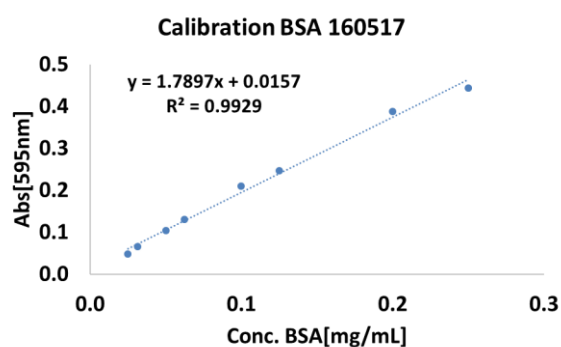
L.O.D[Abs]	L.O.Q[Abs]	L.O.D[mg/mL]	L.O.Q[mg/mL]
0.042	0.077	0.010	2.767



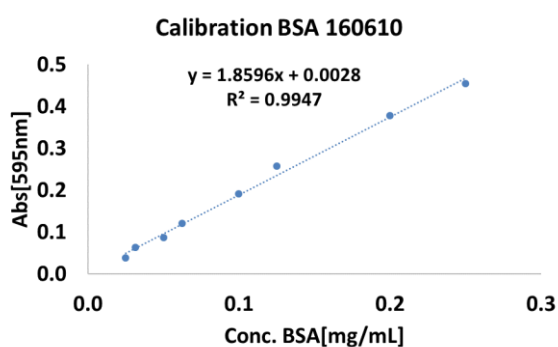
L.O.D[Abs]	L.O.Q[Abs]	L.O.D[mg/mL]	L.O.Q[mg/mL]
0.016	0.049	0.009	1.035



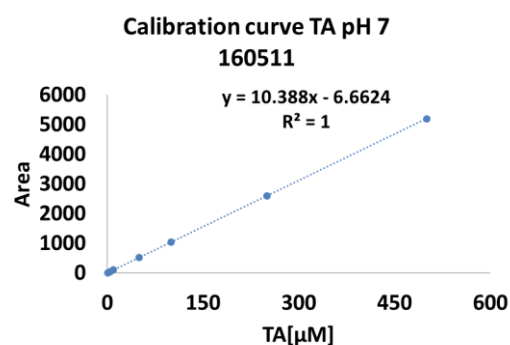
L.O.D[Abs]	L.O.Q[Abs]	L.O.D[mg/mL]	L.O.Q[mg/mL]
0.029	0.066	0.009	0.030



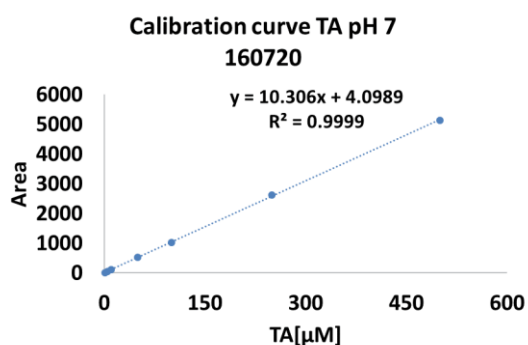
L.O.D[Abs]	L.O.Q[Abs]	L.O.D[mg/mL]	L.O.Q[mg/mL]
0.061	0.177	0.028	0.094



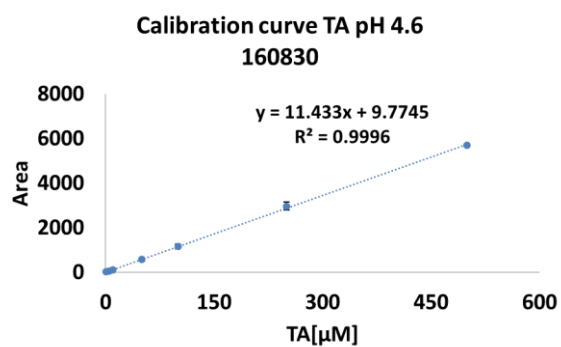
L.O.D[Abs]	L.O.Q[Abs]	L.O.D[mg/mL]	L.O.Q[mg/mL]
0.032	0.071	0.009	0.031



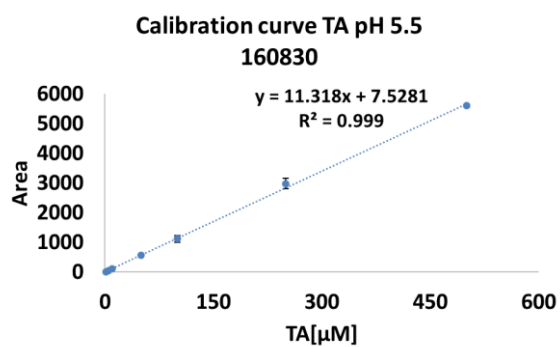
L.O.D[Area]	L.O.D[Area]	L.O.D[μM]	L.O.D[μM]
8.34	12.24	1.4438	1.8195



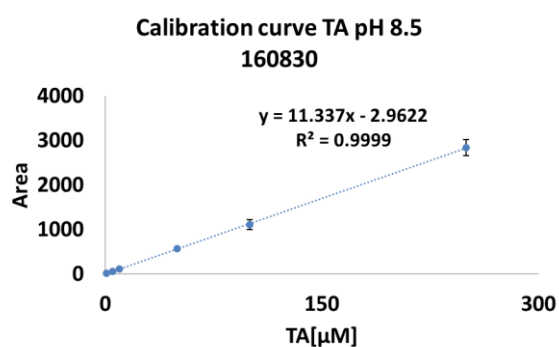
L.O.D[Area]	L.O.Q[Area]	L.O.D[μM]	L.O.Q[μM]
16.94	40.54	1.25	3.54



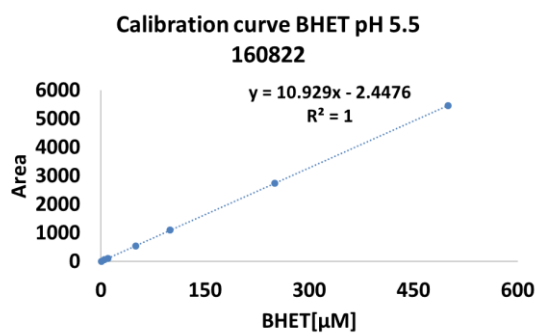
L.O.D[Area]	L.O.Q[Area]	L.O.D[μ M]	L.O.Q[μ M]
11.95	91.26	0.36	7.27



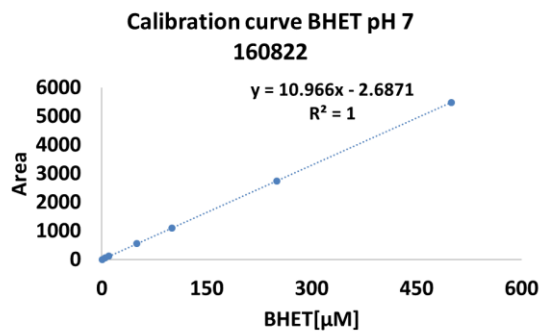
L.O.D[Area]	L.O.Q[Area]	L.O.D[μ M]	L.O.Q[μ M]
58.18	149.69	4.48	12.56



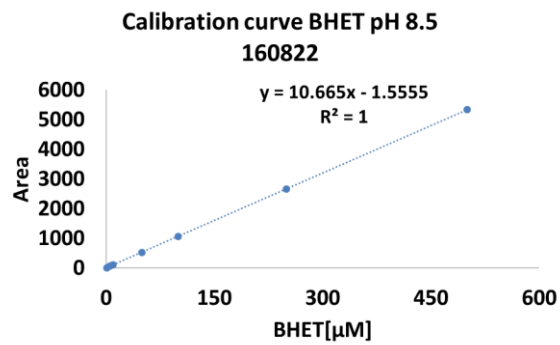
L.O.D[Area]	L.O.Q[Area]	L.O.D[μ M]	L.O.Q[μ M]
3.33	22.25	0.56	2.22



L.O.D[Area]	L.O.Q[Area]	L.O.D[μ M]	L.O.Q[μ M]
8.47	22.54	1.00	2.29

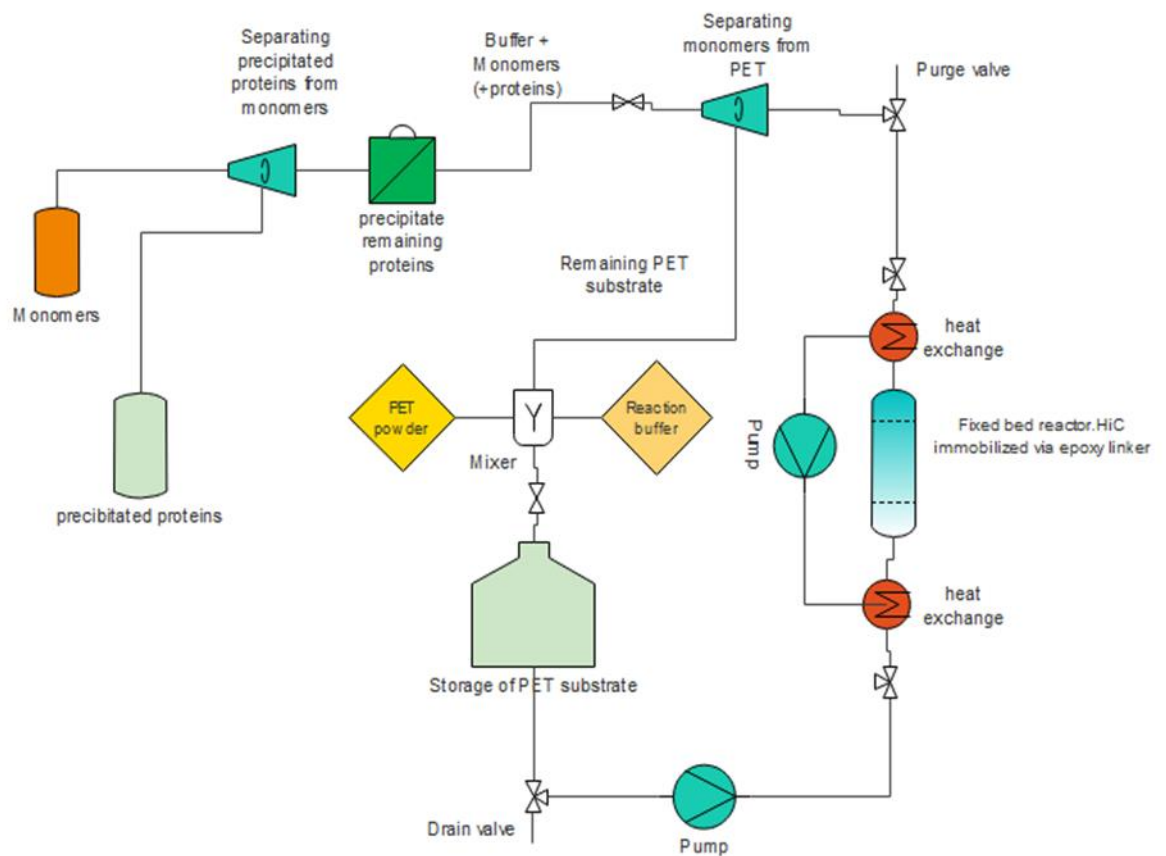


L.O.D[Area]	L.O.Q[Area]	L.O.D[μ M]	L.O.Q[μ M]
9.43	25.71	1.08	2.57



L.O.D[Area]	L.O.Q[Area]	L.O.D[μM]	L.O.Q[μM]
2.29	6.68	0.25	0.67

Process concept for fixed bed enzyme reactor with feed back loop



7. Reference list

- Abo, Masnobu, Morten Wurtz Christensen, and Zhengyu Hu. 2011. "Production of Fatty Acid Alkyl Esters by Use of Two Lipolytic Enzymes." Retrieved August 1, 2017 (<https://www.google.com/patents/US9593352>).
- Al-Sabagh, A. M., F. Z. Yehia, Gh. Eshaq, A. M. Rabie, and A. E. ElMetwally. 2016. "Greener Routes for Recycling of Polyethylene Terephthalate." *Egyptian Journal of Petroleum* 25(1):53–64. Retrieved August 1, 2017 (<http://linkinghub.elsevier.com/retrieve/pii/S1110062115000148>).
- Alvarez-Ordóñez, Avelino and Miguel Prieto. 2012. *Fourier Transform Infrared Spectroscopy in Food Microbiology*. Boston, MA: Springer US. Retrieved November 14, 2016 (<http://link.springer.com/10.1007/978-1-4614-3813-7>).
- Alves, N. M., J. F. Mano, E. Balaguer, J. M. Meseguer Dueñas, and J. L. Gómez Ribelles. 2002. "Glass Transition and Structural Relaxation in Semi-Crystalline Poly(ethylene Terephthalate): A DSC Study." *Polymer* 43(15):4111–22. Retrieved August 15, 2017 (<http://linkinghub.elsevier.com/retrieve/pii/S0032386102002367>).
- Anastas, P. T. and J. C. Warner. 1998. "Green Chemistry: Theory and Practice." *Oxford University Press: New York* p.30.
- Andrigo, P., R. Bagatin, and G. Pagani. 1999. "Fixed Bed Reactors." *Catalysis Today* 52(2):197–221.
- Anon. n.d. "image149.png (716×428)." Retrieved (<http://chem.libretexts.org/@api/deki/files/4078/=image149.png?revision=1>).
- Baker, Peter James, Christopher Poultney, Zhiqiang Liu, Richard Gross, and Jin Kim Montclare. 2012. "Identification and Comparison of Cutinases for Synthetic Polyester Degradation." *Applied Microbiology and Biotechnology* 93(1):229–40.
- de Barros, Dragana P. C., Pedro Fernandes, Joaquim M. S. Cabral, and Luís P. Fonseca. 2011. "Synthetic Application and Activity of Cutinase in an Aqueous, Miniemulsion Model System: Hexyl Octanoate Synthesis." *Catalysis Today* 173(1):95–102. Retrieved March 8, 2016 (<http://www.sciencedirect.com/science/article/pii/S0920586111004731>).
- Barth, Markus et al. 2015. "Effect of Hydrolysis Products on the Enzymatic Degradation of Polyethylene Terephthalate Nanoparticles by a Polyester Hydrolase from *Thermobifida Fusca*." *Biochemical Engineering Journal* 93:222–28. Retrieved August 7, 2017 (<http://linkinghub.elsevier.com/retrieve/pii/S1369703X14002964>).
- Barth, Markus et al. 2016. "A Dual Enzyme System Composed of a Polyester Hydrolase and a Carboxylesterase Enhances the Biocatalytic Degradation of Polyethylene Terephthalate Films." *Biotechnology Journal* 11(8):1082–87. Retrieved August 6, 2017 (<http://doi.wiley.com/10.1002/biot.201600008>).
- Bommarius, A. S. and A. Karau. 2005. "Deactivation of Formate Dehydrogenase (FDH) in Solution and

- at Gas-Liquid Interfaces.” *Biotechnology Progress* 21(6):1663–72. Retrieved August 5, 2017 (<http://doi.wiley.com/10.1021/bp050249q>).
- Braun, Sergei, Sara Rappoport, Rivka Zusman, David Avnir, and Michael Ottolenghi. 1990. “Biochemically Active Sol-Gel Glasses: The Trapping of Enzymes.” *Materials Letters* 10(1–2):1–5. Retrieved August 6, 2017 (<http://linkinghub.elsevier.com/retrieve/pii/0167577X90900024>).
- Brena, Beatriz M. and Francisco Batista-Viera. 2006. “Immobilization of Enzymes.” Pp. 15–30 in. Retrieved April 24, 2017 (http://link.springer.com/10.1007/978-1-59745-053-9_2).
- Brueckner, Tina, Anita Eberl, Sonja Heumann, Maike Rabe, and Georg M. Guebitz. 2008. “Enzymatic and Chemical Hydrolysis of Poly(ethylene Terephthalate) Fabrics.” *Journal of Polymer Science Part A: Polymer Chemistry* 46(19):6435–43. Retrieved April 30, 2017 (<http://doi.wiley.com/10.1002/pola.22952>).
- Brunner, G.(Gerd). 2004. *Supercritical Fluids as Solvents and Reaction Media*. Elsevier.
- Cantone, Sara et al. 2013. “Efficient Immobilisation of Industrial Biocatalysts: Criteria and Constraints for the Selection of Organic Polymeric Carriers and Immobilisation Methods.” *Chemical Society Reviews* 42(15):6262. Retrieved March 8, 2016 (<http://xlink.rsc.org/?DOI=c3cs35464d>).
- Carvalho, Cristina M. L., Maria Raquel Aires-Barros, and Joaquim M. S. Cabral. 1998. “Cutinase Structure, Function and Biocatalytic Applications.” *EJB Electronic Journal of Biotechnology* 1(3):717–345. Retrieved February 17, 2017 (<http://www.ist.utl.pt/>).
- Caussette, Mylène, Alain Gaunand, Henri Planche, and Brigitte Lindet. 1998. “Enzyme Inactivation by Inert Gas Bubbling.” Pp. 393–98 in. Retrieved August 5, 2017 (<http://linkinghub.elsevier.com/retrieve/pii/S0921042398800579>).
- Dalpozzo, Renato et al. 2015. “Magnetic Nanoparticle Supports for Asymmetric Catalysts.” *Green Chem.* 17(7):3671–86. Retrieved January 15, 2017 (<http://xlink.rsc.org/?DOI=C5GC00386E>).
- Damborsky, J. and J. Koca. 1999. “Analysis of the Reaction Mechanism and Substrate Specificity of Haloalkane Dehalogenases by Sequential and Structural Comparisons.” *Protein Engineering Design and Selection* 12(11):989–98. Retrieved February 21, 2017 (<https://academic.oup.com/peds/article-lookup/doi/10.1093/protein/12.11.989>).
- Daouk, Elias et al. 2017. “Oxidative Pyrolysis of Wood Chips and of Wood Pellets in a Downdraft Continuous Fixed Bed Reactor.” *Fuel* 196:408–18. Retrieved April 28, 2017 (<http://www-1sciencedirect-1com-1bokusummon.piscis.boku.ac.at/science/article/pii/S0016236117301564>).
- Datta, Sumitra, L.Rene Christena, and Yamuna Rani Sriramulu Rajaram. 2013. “Enzyme Immobilization: An Overview on Techniques and Support Materials.” *3 Biotech* 3(1):1–9. Retrieved March 8, 2016 (<http://link.springer.com/10.1007/s13205-012-0071-7>).
- Demertzis, P. G., F. Johansson, C. Lievens, and R. Franz. 1997. “Studies on the Development of a Quick Inertness Test Procedure for Multi-Use PET Containers—sorption Behaviour of Bottle Wall Strips.” *Packaging Technology and Science* 10(1):45–58. Retrieved August 1, 2017

- (<http://doi.wiley.com/10.1002/%28SICI%291099-1522%28199701/02%2910%3A1%3C45%3A%3AAID-PTS383%3E3.0.CO%3B2-L>).
- Fetzner, Susanne and Roberto A. Steiner. 2010. "Cofactor-Independent Oxidases and Oxygenases." *Applied Microbiology and Biotechnology* 86(3):791–804. Retrieved February 21, 2017 (<http://link.springer.com/10.1007/s00253-010-2455-0>).
- Firth, Benjamin, Stan T. Kolaczowski, Matthew G. Davidson, Serpil Awdry, and web-support@bath.ac.uk. 2012. "Biodiesel Production in Fixed-Bed Catalytic Reactors." Retrieved April 29, 2017 (<http://opus.bath.ac.uk/34788/>).
- Flipsen, J. A. C., A. C. M. Appel, H. T. W. M. van der Hijden, and C. T. Verrips. 1998. "Mechanism of Removal of Immobilized Triacylglycerol by Lipolytic Enzymes in a Sequential Laundry Wash Process." *Enzyme and Microbial Technology* 23(3):274–80.
- Flipsen, J. A., H. T. van der Hijden, M. R. Egmond, and H. M. Verheij. 1996. "Action of Cutinase at the Triolein-Water Interface. Characterisation of Interfacial Effects during Lipid Hydrolysis Using the Oil-Drop Tensiometer as a Tool to Study Lipase Kinetics." *Chemistry and Physics of Lipids* 84(2):105–15. Retrieved February 19, 2017 (<http://www.ncbi.nlm.nih.gov/pubmed/9081775>).
- Franken, S. M., H. J. Rozeboom, K. H. Kalk, and B. W. Dijkstra. 1991. "Crystal Structure of Haloalkane Dehalogenase: An Enzyme to Detoxify Halogenated Alkanes." *The EMBO Journal* 10(6):1297–1302. Retrieved February 21, 2017 (<http://www.ncbi.nlm.nih.gov/pubmed/2026135>).
- Genencor. 1988. "Increasing Pharmacological Effect of Agricultural Chemicals."
- Giannotta, Giorgio et al. 1994. "Processing Effects on Poly(ethylene Terephthalate) from Bottle Scraps." *Polymer Engineering and Science* 34(15):1219–23. Retrieved August 1, 2017 (<http://doi.wiley.com/10.1002/pen.760341508>).
- Gomes, Daniela, Teresa Matamá, Artur Cavaco-Paulo, Galba Takaki, and Alexandra Salgueiro. 2013. "Production of Heterologous Cutinases by E. Coli and Improved Enzyme Formulation for Application on Plastic Degradation." *Electronic Journal of Biotechnology* 16(5). Retrieved April 28, 2017 (<http://www.ejbiotechnology.info/index.php/ejbiotechnology/article/view/1368>).
- Gonçalves, A. P. V., J. M. S. Cabral, and M. R. Aires-Barros. 1996. "Immobilization of a Recombinant Cutinase by Entrapment and by Covalent Binding." *Applied Biochemistry and Biotechnology* 60(3):217–28. Retrieved February 19, 2017 (<http://link.springer.com/10.1007/BF02783585>).
- Goodfellow Inc. 2003. "Polyethylene Terephthalate Polyester (PET , PETP) - Properties and Applications - Supplier Data by Goodfellow." 1–6. Retrieved January 11, 2017 (<http://www.azom.com/article.aspx?ArticleID=2047>).
- Grochulski, Paweł et al. 1993. "Insights into Interfacial Activation from an Open Structure of Candida Rugosa Lipase." *Journal of Biological Chemistry* 268(17):12843–47.
- Guebitz, Georg M. and Artur Cavaco-Paulo. 2008. "Enzymes Go Big: Surface Hydrolysis and Functionalisation of Synthetic Polymers." *Trends in Biotechnology* 26(1):32–38. Retrieved August

- 1, 2017 (<http://linkinghub.elsevier.com/retrieve/pii/S0167779907002879>).
- Harder, Robin et al. 2014. “Quantification of Goods Purchases and Waste Generation at the Level of Individual Households.” *Journal of Industrial Ecology* 18(2):227–41. Retrieved August 6, 2017 (<http://dx.doi.org/10.1111/jiec.12111>).
- Herrero Acero, Enrique et al. 2011. “Enzymatic Surface Hydrolysis of PET: Effect of Structural Diversity on Kinetic Properties of Cutinases from Thermobifida.” *Macromolecules* 44(12):4632–40. Retrieved March 8, 2016 (<http://pubs.acs.org/doi/abs/10.1021/ma200949p>).
- HITACHI. 1994. “Production Process for Polyethylene Terephthalate (PET).” *Industrial Plant Systems*. Retrieved February 20, 2017 (<http://www.hitachi-pt.com/products/ip/process/pet.html>).
- Holmquist, Mats. 2000. “Alpha Beta-Hydrolase Fold Enzymes Structures, Functions and Mechanisms.” *Current Protein and Peptide Science* 1(2):209–35. Retrieved (<http://www.ingentaselect.com/rpsv/cgi-bin/cgi?ini=xref&body=linker&reqdoi=10.2174/1389203003381405>).
- Höök, Mikael, Junchen Li, Kersti Johansson, and Simon Snowden. 2012. “Growth Rates of Global Energy Systems and Future Outlooks.” *Natural Resources Research* 21(1):23–41. Retrieved January 21, 2017 (<http://link.springer.com/10.1007/s11053-011-9162-0>).
- Höök, Mikael, Anders Sivertsson, and Kjell Aleklett. 2010. “Validity of the Fossil Fuel Production Outlooks in the IPCC Emission Scenarios.” *Natural Resources Research* 19(2):63–81. Retrieved January 21, 2017 (<http://link.springer.com/10.1007/s11053-010-9113-1>).
- Huybrechts, Ward, Jérôme Mijoin, Pierre A. Jacobs, and Johan A. Martens. 2003. “Development of a Fixed-Bed Continuous-Flow High-Throughput Reactor for Long-Chain N-Alkane Hydroconversion.” *Applied Catalysis A: General* 243(1):1–13. Retrieved April 28, 2017 (<http://www-1sciencedirect-1com-1bokusummon.pisces.boku.ac.at/science/article/pii/S0926860X02005367>).
- Ibarra, David, M. Concepción Monte, Angeles Blanco, Angel T. Martínez, and María J. Martínez. 2012. “Enzymatic Deinking of Secondary Fibers: Cellulases/hemicellulases versus Laccase-Mediator System.” *Journal of Industrial Microbiology & Biotechnology* 39(1):1–9. Retrieved September 5, 2017 (<http://www.ncbi.nlm.nih.gov/pubmed/21643708>).
- Jaeger, K. E., B. W. Dijkstra, and M. T. Reetz. 1999. “Bacterial Biocatalysts: Molecular Biology, Three-Dimensional Structures, and Biotechnological Applications of Lipases.” *Annual Review of Microbiology* 53(1):315–51. Retrieved April 16, 2017 (<http://www.annualreviews.org/doi/10.1146/annurev.micro.53.1.315>).
- Jaeger, Karl-Erich and Manfred T. Reetz. 1998. “Microbial Lipases Form Versatile Tools for Biotechnology.” *Trends in Biotechnology* 16(9):396–403. Retrieved April 16, 2017 (<http://www-1sciencedirect-1com-1bokusummon.pisces.boku.ac.at/science/article/pii/S0167779998011950>).
- Jeffree, C. .. 1996. “Structure and Ontogeny of Plant Cuticles. In Plant Cuticles: An Integrated

- Functional Approach, G. Kerstiens, Ed.” *Oxford, UK: BIOS Scientific Publishers* 33–82.
- Ji, Li Na. 2013. “Study on Preparation Process and Properties of Polyethylene Terephthalate (PET).” *Applied Mechanics and Materials* 312:406–10. Retrieved (<http://www.scientific.net/AMM.312.406>).
- Kallenberg, Agnes I., Fred van Rantwijk, and Roger A. Sheldon. 2005. “Immobilization of Penicillin G Acylase: The Key to Optimum Performance.” *Advanced Synthesis & Catalysis* 347(7–8):905–26. Retrieved March 8, 2016 (<http://doi.wiley.com/10.1002/adsc.200505042>).
- Karayannidis, G. P., A. P. Chatziavgoustis, and D. S. Achilias. 2002. “Poly(ethylene Terephthalate) Recycling and Recovery of Pure Terephthalic Acid by Alkaline Hydrolysis.” *Advances in Polymer Technology* 21(4):250–59. Retrieved July 31, 2017 (<http://doi.wiley.com/10.1002/adv.10029>).
- Kirk, Ole, Torben Vedel Borchert, and Claus Crone Fuglsang. 2002. “Industrial Enzyme Applications.” *Current Opinion in Biotechnology* 13(4):345–51. Retrieved April 25, 2017 (<http://www.ncbi.nlm.nih.gov/pubmed/12323357>).
- Klähn, Marco, Geraldine S. Lim, and Ping Wu. 2011. “How Ion Properties Determine the Stability of a Lipase Enzyme in Ionic Liquids: A Molecular Dynamics Study.” *Physical Chemistry Chemical Physics* 13(41):18647. Retrieved January 10, 2017 (<http://xlink.rsc.org/?DOI=c1cp22056j>).
- Kocabas, A.Merve, Hande Yukseler, Filiz B. Dilek, and Ulku Yetis. 2009. “Adoption of European Union’s IPPC Directive to a Textile Mill: Analysis of Water and Energy Consumption.” *Journal of Environmental Management* 91(1):102–13. Retrieved April 17, 2017 (<http://www.sciencedirect.com/science/article/pii/S0301479709002400>).
- Kolattukudy, P. E. 1985. “Enzymatic Penetration of the Plant Cuticle by Fungal Pathogens.” *Annu. Rev. Phytopathol.* (23):223–250.
- Kold, David et al. 2014. “Thermodynamic and Structural Investigation of the Specific SDS Binding of *Humicola Insolens* Cutinase.” *Protein Science: A Publication of the Protein Society* 23(8):1023–35. Retrieved April 16, 2017 (<http://www.ncbi.nlm.nih.gov/pubmed/24832484>).
- Köpnick, Horst et al. 2000. “Polyesters.” in *Ullmann’s Encyclopedia of Industrial Chemistry*. Weinheim, Germany: Wiley-VCH Verlag GmbH & Co. KGaA. Retrieved August 1, 2017 (http://doi.wiley.com/10.1002/14356007.a21_227).
- Laemmli, U. K. 1970. “Cleavage of Structural Proteins during the Assembly of the Head of Bacteriophage T4.” *Nature* 227(5259):680–85. Retrieved November 14, 2016 (<http://www.ncbi.nlm.nih.gov/pubmed/5432063>).
- Letzel, Hubert Rehm/.Thomas. 2010. *Der Experimentator: Proteinbiochemie/Proteomics*.
- Liao D I and S. J. Remington. 1990. “Structure of Wheat Serine Carboxypeptidase II at 3.5-Å Resolution. A New Class of Serine Proteinase.” *J. Biol. Chem.* 265:6528–31.
- Mariani, Angela M., Mary E. Natoli, and Peter Kofinas. 2013. “Enzymatic Activity Preservation and Protection through Entrapment within Degradable Hydrogels.” *Biotechnology and Bioengineering*

- 110(11):2994–3002. Retrieved August 6, 2017 (<http://doi.wiley.com/10.1002/bit.24971>).
- Mateo, Cesar, Olga Abian, Roberto Fernandez–Lafuente, and Jose M. Guisan. 2000. “Increase in Conformational Stability of Enzymes Immobilized on Epoxy-Activated Supports by Favoring Additional Multipoint Covalent Attachment☆.” *Enzyme and Microbial Technology* 26(7):509–15. Retrieved August 7, 2017 (<http://linkinghub.elsevier.com/retrieve/pii/S014102299900188X>).
- Mateo, Cesar, Jose M. Palomo, Gloria Fernandez-Lorente, Jose M. Guisan, and Roberto Fernandez-Lafuente. 2007. “Improvement of Enzyme Activity, Stability and Selectivity via Immobilization Techniques.” *Enzyme and Microbial Technology* 40(6):1451–63.
- Mueller, Rolf-Joachim. 2006. “Biological Degradation of Synthetic polyesters—Enzymes as Potential Catalysts for Polyester Recycling.” *Process Biochemistry* 41(10):2124–28.
- Mulder, A. et al. 1995. “Anaerobic Ammonium Oxidation Discovered in a Denitrifying Fluidized Bed Reactor.” *FEMS Microbiology Ecology* 16(3):177–84. Retrieved April 28, 2017 (<https://academic.oup.com/femsec/article-lookup/doi/10.1111/j.1574-6941.1995.tb00281.x>).
- Nardini, Marco and W.Dijkstra Bauke. 1999. “ α / β Hydrolase Fold Enzymes : The Family Keeps Growing Marco Nardini and Bauke W Dijkstra *.” *Current Opinion in Structural Biology* 9:732–37.
- Nikolaivits, Efstratios, Georgios Makris, and Evangelos Topakas. 2017. “Immobilization of a Cutinase from *Fusarium Oxysporum* and Application in Pineapple Flavor Synthesis.” *Journal of Agricultural and Food Chemistry* 65(17):3505–11. Retrieved August 1, 2017 (<http://pubs.acs.org/doi/abs/10.1021/acs.jafc.7b00659>).
- Nimchua, Thidarat, Hunsu Punnapayak, and Wolfgang Zimmermann. 2007. “Comparison of the Hydrolysis of Polyethylene Terephthalate Fibers by a Hydrolase from *Fusarium Oxysporum* LCH I and *Fusarium Solani* F. Sp.pisi.” *Biotechnology Journal* 2(3):361–64. Retrieved August 1, 2017 (<http://www.ncbi.nlm.nih.gov/pubmed/17136729>).
- Nob Hill Publishing, LLC. 2016. “Fixed-Bed Catalytic Reactors.” Retrieved April 29, 2017 (<http://jbrwww.che.wisc.edu/home/jbraw/chemreacfun/ch7/slides-masswrxn.pdf>).
- O’Connor, Charmian J. and Irene C. Stockley. 1986. “Studies in Bile Salt Solutions.” *Journal of Colloid and Interface Science* 112(2):497–503. Retrieved April 16, 2017 (<http://linkinghub.elsevier.com/retrieve/pii/0021979786901189>).
- Okkels, J. S. 1997. “Preparing Polypeptide Variants with Improved Functional Properties.”
- Ollis, D. L. et al. 1992. “The Alpha/beta Hydrolase Fold.” *Protein Engineering* 5(3):197–211. Retrieved February 21, 2017 (<http://www.ncbi.nlm.nih.gov/pubmed/1409539>).
- Ollis, David L. et al. 1990. “The α / β 3 Hydrolase Fold.” 5(1989):197–211.
- Pang, K., R. Kotek, and A. Tonelli. 2006. “Review of Conventional and Novel Polymerization Processes for Polyesters.” *Progress in Polymer Science (Oxford)* 31(11):1009–37.
- Pathak, D. and D. Ollis. 1990. “Refined Structure of Dienelactone Hydrolase at 1.8 Å.” *Journal of*

- Molecular Biology* 214(2):497–525. Retrieved February 21, 2017 (<http://www.ncbi.nlm.nih.gov/pubmed/2380986>).
- Pellis, A. et al. 2016. “Enlarging the Tools for Efficient Enzymatic Polycondensation: Structural and Catalytic Features of Cutinase 1 from *Thermobifida Cellulosilytica*.” *Catal. Sci. Technol.* Retrieved March 8, 2016 (<http://xlink.rsc.org/?DOI=C5CY01746G>).
- Pellis, Alessandro et al. 2015. “Biocatalyzed Approach for the Surface Functionalization of poly(L-Lactic Acid) Films Using Hydrolytic Enzymes.” *Biotechnology Journal* 10(11):1739–49. Retrieved March 8, 2016 (<http://doi.wiley.com/10.1002/biot.201500074>).
- Pellis, Alessandro, Enrique Herrero Acero, et al. 2016. “The Closure of the Cycle: Enzymatic Synthesis and Functionalization of Bio-Based Polyesters.” *Trends in Biotechnology* 34(4):316–28. Retrieved August 1, 2017 (<http://linkinghub.elsevier.com/retrieve/pii/S0167779915002693>).
- Pellis, Alessandro, Caroline Gamerith, et al. 2016. “Ultrasound-Enhanced Enzymatic Hydrolysis of Poly(ethylene Terephthalate).” *Bioresource Technology* (August). Retrieved (<http://www.sciencedirect.com/science/article/pii/S0960852416310859>).
- Pellis, Alessandro, Marco Vastano, Felice Quartinello, Enrique Herrero Acero, and Georg M. Guebitz. 2017. “His-Tag Immobilization of Cutinase 1 from *Thermobifida Cellulosilytica* for Solvent-Free Synthesis of Polyesters.” *Biotechnology Journal* 1700268. Retrieved August 1, 2017 (<http://doi.wiley.com/10.1002/biot.201700322>).
- Petersen, Steffen B., Peter Fojan, Evamaria I. Petersen, and Maria Teresa Neves Petersen. 2001. “The Thermal Stability of the *Fusarium Solani* Pisi Cutinase as a Function of pH.” *Journal of Biomedicine and Biotechnology* 2001(2):62–69.
- Pratima Bajpai. n.d. *Green Chemistry and Sustainability in Pulp and Paper Industry - Pratima Bajpai - Google Books*. Springer. Retrieved April 29, 2017 (<https://books.google.at/books?id=WbT-CQAAQBAJ&pg=PA196&lpg=PA196&dq=green+chemistry+fixed+bed+reactor&source=bl&ots=JQakvhvkLw&sig=ZudZltiTT0ABzTQuq4pr93CIxFU&hl=de&sa=X&ved=0ahUKEwj0nbXV8snTAhXEIsAKHRRCBMYQ6AEIOzAC#v=onepage&q=green%2520chemistry%2520fixed%2520>).
- Purdy, R. E. and P. E. Kolattukudy. 1975. “Hydrolysis of Plant Cuticle by Plant Pathogens. Properties of Cutinase I, Cutinase II, and a Nonspecific Esterase Isolated from *Fusarium Solani* Pisi.” *Biochemistry* 14(13):2832–2840. Retrieved March 8, 2016 (<http://pubs.acs.org/doi/abs/10.1021/bi00684a007>).
- Quartinello, Felice et al. 2017. “Synergistic Chemo-Enzymatic Hydrolysis of Poly(ethylene Terephthalate) from Textile Waste.” *Microbial Biotechnology* 0.
- Reetz, Manfred T. 1997. “Entrapment of Biocatalysts in Hydrophobic Sol-Gel Materials for Use in Organic Chemistry.” *Advanced Materials* 9(12):943–54. Retrieved August 6, 2017 (<http://doi.wiley.com/10.1002/adma.19970091203>).

- Resyntex. 2017. "The Project | Resyntex." Retrieved April 23, 2017 (<http://www.resyntex.eu/the-project>).
- Ribitsch, Doris et al. 2012. "A New Esterase from Thermobifida Halotolerans Hydrolyses Polyethylene Terephthalate (PET) and Polylactic Acid (PLA)." *Polymers* 4(1):617–29. Retrieved March 8, 2016 (<http://www.mdpi.com/2073-4360/4/1/617>).
- Ronkvist, Åsa M., Wenchun Xie, Wenhua Lu, and Richard A. Gross. 2009. "Cutinase-Catalyzed Hydrolysis of Poly(ethylene Terephthalate)." *Macromolecules* 42(14):5128–38. Retrieved August 1, 2017 (<http://pubs.acs.org/doi/abs/10.1021/ma9005318>).
- Saito, Shogo and Tatsuji Nakajima. 1959. "Glass Transition in Polymers." *Journal of Applied Polymer Science* 2(4):93–99. Retrieved August 13, 2017 (<http://doi.wiley.com/10.1002/app.1959.070020414>).
- Schrag, Joseph D., Yunge Li, Shan Wu, and Mirosław Cygler. 1991. "Ser-His-Glu Triad Forms the Catalytic Site of the Lipase from *Geotrichum Candidum*." *Nature* 351(6329):761–64. Retrieved February 21, 2017 (<http://www.ncbi.nlm.nih.gov/pubmed/2062369>).
- Sebastião, M. J., J. M. S. Cabral, and M. R. Aires-Barros. 1993. "Synthesis of Fatty Acid Esters by a Recombinant Cutinase in Reversed Micelles." *Biotechnology and Bioengineering* 42(3):326–32. Retrieved February 19, 2017 (<http://www.ncbi.nlm.nih.gov/pubmed/18613016>).
- Sheldon, Roger A. 2007. "Enzyme Immobilization: The Quest for Optimum Performance." *Advanced Synthesis & Catalysis* 349(8–9):1289–1307. Retrieved March 8, 2016 (<http://doi.wiley.com/10.1002/adsc.200700082>).
- Shen, Qiuyun et al. 2011. "Gelatin-Templated Biomimetic Calcification for β -Galactosidase Immobilization." *Process Biochemistry* 46(8):1565–71. Retrieved August 6, 2017 (<http://linkinghub.elsevier.com/retrieve/pii/S135951131100153X>).
- Silva, D. A. et al. 2005. "Degradation of Recycled PET Fibers in Portland Cement-Based Materials." *Cement and Concrete Research* 35(9):1741–46.
- Sinha, Vijaykumar, Mayank R. Patel, and Jigar V. Patel. 2010. "Pet Waste Management by Chemical Recycling: A Review." *Journal of Polymers and the Environment* 18(1):8–25. Retrieved April 16, 2017 (<http://link.springer.com/10.1007/s10924-008-0106-7>).
- Soumanou, Mohamed M. and Uwe T. Bornscheuer. 2003. "Lipase-Catalyzed Alcoholysis of Vegetable Oils." *European Journal of Lipid Science and Technology* 105(11):656–60. Retrieved August 5, 2017 (<http://doi.wiley.com/10.1002/ejlt.200300871>).
- Steiner, Roberto A., Helge J. Janssen, Pietro Roversi, Aaron J. Oakley, and Susanne Fetzner. 2010. "Structural Basis for Cofactor-Independent Dioxygenation of N-Heteroaromatic Compounds at the Alpha/beta-Hydrolase Fold." *Proceedings of the National Academy of Sciences of the United States of America* 107(2):657–62. Retrieved February 21, 2017 (<http://www.ncbi.nlm.nih.gov/pubmed/20080731>).

- Su, Lingqia, Ruoyu Hong, Xiaojie Guo, Jing Wu, and Yongmei Xia. 2016. "Short-Chain Aliphatic Ester Synthesis Using *Thermobifida Fusca* Cutinase." *Food Chemistry* 206:131–36. Retrieved August 1, 2017 (<http://linkinghub.elsevier.com/retrieve/pii/S0308814616304046>).
- Sussman, J. L. et al. 1991. "Atomic Structure of Acetylcholinesterase from *Torpedo Californica*: A Prototypic Acetylcholine-Binding Protein." *Science (New York, N.Y.)* 253(5022):872–79. Retrieved February 21, 2017 (<http://www.ncbi.nlm.nih.gov/pubmed/1678899>).
- Tasca, Federico et al. 2010. "Increasing the Coulombic Efficiency of Glucose Biofuel Cell Anodes by Combination of Redox Enzymes." *Biosensors and Bioelectronics* 25(7):1710–16. Retrieved August 1, 2017 (<http://linkinghub.elsevier.com/retrieve/pii/S095656630900668X>).
- Tischer, W. and V. Kascher. 1999. "No Title." *Trends in Biotechnology* 17:326–35.
- Toshiaki Yoshioka, *, and Tsutomu Motoki, and Akitsugu Okuwaki. 2000. "Kinetics of Hydrolysis of Poly(ethylene Terephthalate) Powder in Sulfuric Acid by a Modified Shrinking-Core Model." Retrieved August 1, 2017 (<http://pubs.acs.org/doi/abs/10.1021/ie000592u>).
- Tyndall, Joel D. A., Supachok Sinchaikul, Linda A. Fothergill-gilmore, Paul Taylor, and Malcolm D. Walkinshaw. 2002. "Crystal Structure of a Thermostable Lipase from *Bacillus Stearotherophilus* P1." 2836(2):859–69.
- Tyndall, Joel D. A., Supachok Sinchaikul, Linda A. Fothergill-Gilmore, Paul Taylor, and Malcolm D. Walkinshaw. 2002. "Crystal Structure of a Thermostable Lipase from *Bacillus Stearotherophilus* P1." *Journal of Molecular Biology* 323(5):859–69. Retrieved April 16, 2017 (<http://www.sciencedirect.com/science/article/pii/S0022283602010045>).
- Unilever. 1994. "Eukaryotic Cutinase Variant with Increased Lipolytic Activity."
- Wang, Youjiang. 2010. "Fiber and Textile Waste Utilization." *Waste and Biomass Valorization* 1(1):135–43. Retrieved April 16, 2017 (<http://link.springer.com/10.1007/s12649-009-9005-y>).
- Waters. 2017. "HPLC System : Waters." Retrieved (http://www.waters.com/waters/de_DE/How-Does-High-Performance-Liquid-Chromatography-Work%3F/nav.htm?cid=10049055&locale=de_DE).
- Webb, Hayden, Jaimys Arnott, Russell Crawford, and Elena Ivanova. 2012. "Plastic Degradation and Its Environmental Implications with Special Reference to Poly(ethylene Terephthalate)." *Polymers* 5(1):1–18. Retrieved January 16, 2017 (<http://www.mdpi.com/2073-4360/5/1/1/>).
- Wei, Ren et al. 2016. "Engineered Bacterial Polyester Hydrolases Efficiently Degrade Polyethylene Terephthalate due to Relieved Product Inhibition." *Biotechnology and Bioengineering* 113(8):1658–65.
- Wei, Ren, Thorsten Oeser, Susan Billig, and Wolfgang Zimmermann. 2012. "A High-Throughput Assay for Enzymatic Polyester Hydrolysis Activity by Fluorimetric Detection." *Biotechnology Journal* 7(12):1517–21. Retrieved August 15, 2017 (<http://www.ncbi.nlm.nih.gov/pubmed/22623363>).
- Wiles, Charlotte et al. 2014. "Continuous Process Technology: A Tool for Sustainable Production." *Green Chem.* 16(1):55–62. Retrieved January 24, 2017 (<http://xlink.rsc.org/?DOI=C3GC41797B>).

- Würtz Christensen, Morten, Lotte Andersen, Tommy Lykke Husum, and Ole Kirk. 2003. "Industrial Lipase Immobilization." *European Journal of Lipid Science and Technology* 105(6):318–21. Retrieved April 25, 2017 (<http://doi.wiley.com/10.1002/ejlt.200390062>).
- Yeats, T. H. and J. K. C. Rose. 2013. "The Formation and Function of Plant Cuticles." *PLANT PHYSIOLOGY* 163(1):5–20. Retrieved February 19, 2017 (<http://www.ncbi.nlm.nih.gov/pubmed/23893170>).
- Yoshida, Shosuke et al. 2016. "A Bacterium That Degrades and Assimilates Poly(ethylene Terephthalate)." *Science* 351(6278). Retrieved August 1, 2017 (<http://science.sciencemag.org/content/351/6278/1196.full>).
- Zimmermann, Wolfgang and Susan Billig. 2010. "Enzymes for the Biofunctionalization of Poly(Ethylene Terephthalate)." Pp. 97–120 in. Springer, Berlin, Heidelberg. Retrieved July 31, 2017 (http://link.springer.com/10.1007/10_2010_87).